



Impacts of future agricultural change on ecosystem service indicators

Sam S. Rabin¹, Peter Alexander^{2,3}, Roslyn Henry², Peter Anthoni¹, Thomas A. M. Pugh^{4,5}, Mark Rounsevell¹, and Almut Arneth¹

¹Institute of Meteorology and Climate Research / Atmospheric Environmental Research, Karlsruhe Institute of Technology, Germany

²School of Geosciences, University of Edinburgh, UK

³Global Academy of Agriculture and Food Security, The Royal (Dick) School of Veterinary Studies, University of Edinburgh, UK

⁴School of Geography, Earth and Environmental Sciences, University of Birmingham, UK

⁵Birmingham Institute of Forest Research, University of Birmingham, UK

Correspondence: Sam S. Rabin (sam.rabin@kit.edu)

Abstract. A future of increasing atmospheric carbon dioxide concentrations, changing climate, growing human populations, and shifting socioeconomic conditions means that the global agricultural system will need to adapt in order to feed the world. These changes will affect not only agricultural land, but terrestrial ecosystems in general. Here, we use the coupled land use and vegetation model LandSyMM to quantify future land use change and resulting impacts on ecosystem service indicators including carbon sequestration, runoff, and nitrogen pollution. We additionally hold certain variables, such as climate or land use, constant to assess the relative contribution of different drivers to the projected impacts. While indicators of some ecosystem services (e.g., flood and drought risk) see trends that are mostly dominated by the direct effects of climate change, others (e.g., carbon sequestration) depend critically on land use and management. Scenarios in which climate change mitigation is more difficult (Shared Socioeconomic Pathways 3 and 5) have the strongest impacts on ecosystem service indicators, such as a loss of 13–19% of land in biodiversity hotspots and a 28% increase in nitrogen pollution. Evaluating a suite of ecosystem service indicators across scenarios enables the identification of tradeoffs and co-benefits associated with different climate change mitigation and adaptation strategies and socioeconomic developments.

1 Introduction

Exploring how the agricultural system might shift under different plausible future climate and socioeconomic changes is critically important for understanding how the future world—with a population in 2100 larger than today's by anywhere from 1.5 billion to nearly 6 billion people (KC and Lutz, 2017)—will be fed. However, the implications of changing agricultural land area and management inputs go far beyond food security. The conversion of forests and other ecosystems to croplands or pasture—combined with the inputs required to produce food on those lands—emits large amounts of greenhouse gases, reduces the ability of the natural world to buffer against anthropogenic carbon dioxide emissions, results in pollution of important freshwater and marine ecosystems, harms biodiversity, and affects water availability and flood risk. Such impacts are not



merely academic, because they affect the livelihoods of human societies which depend on a wide range of ecosystem services which broadly fall into three categories (IPBES, 2018a): regulating (e.g., greenhouse gas sequestration, flood control), material (e.g., food and feed production), and non-material (e.g., learning and inspiration). As global environmental and societal changes continue to accelerate over the coming decades, it is critical that we understand not just the impacts on the natural world, but
25 how those impacts feed back onto humanity.

To explore the possible future evolution of the Earth system and society, models have been developed that simulate the global economy, natural world, and their interactions. A substantial body of research has been built up using such models to examine how future land-use change will affect individual ecosystem services such as carbon sequestration (Brovkin et al., 2013; Lawrence et al., 2018), biodiversity (Jantz et al., 2015; Hof et al., 2018; Di Marco et al., 2019), and water availability and
30 flood risk (Davie et al., 2013; Elliott et al., 2014; Asadieh and Krakauer, 2017). Much less work has been undertaken to evaluate the future of a suite of ecosystem services in an integrated way (Krause et al., 2017; Molotoks et al., 2018). However, such analyses provide critically important evidence for balancing the many competing demands on the land system while achieving climate and societal targets such as those laid out in the Paris Agreement and Sustainable Development goals (Eitelberg et al., 2016; Benton et al., 2018; Verhagen et al., 2018).

Previously, we used the PLUM land-use model to estimate future land use and management change, based on changing socio-economic conditions as well as climate effects on agricultural yield provided by the vegetation model LPJ-GUESS (Alexander et al., 2018). This coupled model system—the Land System Modular Model, or LandSyMM—is unique among global land-use change models in the high level of spatial detail that it considers in the response of agricultural yields to management inputs, as well as in allowing short-term over- and under-supply of commodities relative to demand (rather than assuming
40 market equilibrium in every year). Here, we take advantage of the mechanistic modeling of terrestrial ecosystems provided by LPJ-GUESS to explore how PLUM-generated future land use and management trajectories—under different scenarios of future socioeconomic development and climate change—differ in their consequences for a range of regulating and material ecosystem services.

2 Methods

45 2.1 LPJ-GUESS and ecosystem services

The Lund-Potsdam-Jena General Ecosystem Simulator (LPJ-GUESS) is a dynamic global vegetation model that simulates—here, at a spatial resolution of 0.5 degrees—physiological, demographic, and disturbance processes among a variety of plant functional types (PFTs) on natural land (Smith et al., 2001, 2014). Agricultural land is also included, with cropland and pasture being restricted in the types of plants allowed and experiencing annual harvest. Transitions among land use types are given
50 as an input, with LPJ-GUESS calculating the associated change in carbon pools and fluxes (Lindeskog et al., 2013). Four crop functional types (CFTs) are represented: C₃ cereals sown in winter and spring, C₄ cereals, and rice (Olin et al., 2015a). Nitrogen limitation on plant growth is modeled, with cropland able to receive fertilizer applications (Smith et al., 2014; Olin et al., 2015b). The mechanistic representation of wild plant and crop growth accounts for the CO₂ fertilization effect, by which



productivity can be enhanced due to improved water use efficiency and (in C_3 plants) reduced photorespiration (Smith et al.,
55 2014). Changes to irrigation, water demand, water supply, and plant water stress as described in the Supplementary Information
of Alexander et al. (2018) were included.

LPJ-GUESS simulates indicators of a number of provisioning and regulating ecosystem services (see also Table 1 in Krause
et al. (2017)). Along with providing some background information, the rest of this section will detail the relevant LPJ-GUESS
60 outputs for the ecosystem service indicators analyzed in this paper having to do with carbon sequestration, water supply,
nitrogen pollution, biogenic volatile organic compounds (BVOCs), and biodiversity.

The conversion of forests and other ecosystems to croplands or pasture has been responsible for about a third of humanity's
CO₂ emissions since 1750. Land clearance for agriculture affects carbon storage by emitting vegetation and soil carbon from
existing pools, as well as by reducing sequestration potential (Ciais et al., 2013). Land-based mitigation strategies—including
reducing deforestation, increasing sequestration in natural and agricultural lands, and expanding biofuels' contribution to en-
65 ergy supply—could play a critical role in whether warming targets laid out in the Paris Agreement can actually be achieved
(Rogelj et al., 2018; van Vuuren et al., 2018). The change in total carbon stored in the land system is used here as a measure of
the carbon sequestration performed by terrestrial ecosystems.

Land use and management change can also impact how ecosystems regulate water quantity, quality, and flood risk (Wheater
and Evans, 2009; Haddeland et al., 2014). Land use change affects runoff by changing how vegetation intercepts rainfall and
70 takes up water from the soil. We consider average annual runoff as it contributes to water levels in lakes and rivers, which is
important for not only freshwater ecosystems but also water availability for irrigation and other human uses (Davie et al., 2013).
After Asadieh and Krakauer (2017), we also use the difference between 1971–2000 and 2071–2100 in the 95th percentile of
monthly surface runoff ($P_{95_{\text{month}}}$) as a proxy for changing flood risk (although note that those authors used daily values), and
the difference in the 5th annual percentile ($P_{5_{\text{year}}}$) for changing drought risk. Note that we are referring to hydrologic drought,
75 which can be contrasted with, e.g., meteorological or socioeconomic drought (Wilhite and Glantz, 1985).

Crop fertilization is the main anthropogenic source of nitrous oxide (N₂O), a potent greenhouse gas responsible for the
third-largest contribution of anthropogenic climate change (Fowler et al., 2009; Myhre et al., 2013; Shcherbak et al., 2014).
Some is also emitted as nitric oxides (NO_x), which contribute to respiratory illnesses via surface-level air pollution (Yang
and Omaye, 2009). Dissolved nitrogen compounds leach from agricultural land into freshwater and marine ecosystems, where
80 they can contribute to their degradation via eutrophication and affect various ecosystem services, including fishery production
(Vitousek et al., 1997). Here, we examine total nitrogen loss from terrestrial ecosystems as output by LPJ-GUESS.

Ecosystem services related to climate change and human health can be strongly affected by biogenic volatile organic com-
pounds (BVOCs), which are emitted by plants—especially woody species (Rosenkranz et al., 2014)—for a variety of phys-
iological functions. In regions where nitrogen oxides are elevated, their reactions with BVOCs produce tropospheric ozone,
85 which is harmful to human health (Ebi and McGregor, 2008), can negatively affect photosynthesis (Ashmore, 2005), and is a
greenhouse gas (Myhre et al., 2013). BVOCs also warm the planet by increasing methane lifetime (Young et al., 2009), but on
the other hand they help form tropospheric aerosols, which increase reflectance and boost photosynthesis via diffuse radiation
(Rap et al., 2018; Sporre et al., 2019). The latter can improve crop yields, but BVOC-enhanced ozone formation can work



90 against that effect (Feng and Kobayashi, 2009). LPJ-GUESS simulates the emission of isoprene and monoterpenes—the most prevalent BVOCs in the atmosphere (Kesselmeier and Staudt, 1999)—and accounts for three important factors regulating their emission: temperature, CO₂ concentration ([CO₂]), and changing distribution of woody plant species due to climate and land use change (Arneeth et al., 2007; Schurgers et al., 2009; Hantson et al., 2017).

Biodiversity underpins a wide range of ecosystem services due to its importance for ecosystem functioning (Tilman et al., 2014) and the possible use of wild species in improving crops (Castañeda-Álvarez et al., 2016) and developing new medicines (Simpson et al., 1996). Land clearance has also been—and will continue to be—responsible for declining biodiversity due to the loss and degradation of habitat (Jantz et al., 2015; Newbold et al., 2015). In addition to raising moral and ethical questions regarding extinction, this negatively impacts ecosystem services and thus people’s livelihoods (IPBES, 2018b). Here we assess how much land is converted to agriculture within the Conservation International (CI) hotspots, a set of 35 regions covering less than 3% of the Earth’s land area but containing half the world’s endemic plant species and over 40% of the world’s endemic 100 vertebrate animal species (Myers et al., 2000; Mittermeier et al., 2004; Henry et al., 2019). These regions each contain at least 1500 endemic vascular plant species and have already lost at least 70% of their original natural vegetation, thus representing highly diverse areas presently at high risk of habitat loss.

2.2 PLUM

The Parsimonious Land Use Model (PLUM) is designed to produce trajectories of land use and management based on socioeconomic trends and gridcell-level crop and pasture productivity at a resolution of 0.5 degrees (Engström et al., 2016b; 105 Alexander et al., 2018). Food demand is projected into the future based on the Shared Socioeconomic Pathway (SSP) scenarios (O’Neill et al., 2014; IIASA, 2014), using the historical relationship of per capita GDP to consumption of each of six crop types—C₃ cereals, C₄ cereals, rice, oilcrops, pulses, and starchy roots—plus ruminant and monogastric livestock (FAOSTAT, 2018a, b). Demand of a seventh crop type—dedicated bioenergy crops such as *Miscanthus*—is specified according to the SSP2 110 scenario described by Popp et al. (2017); demand for bioenergy from food crops is specified to double from 2010 by 2030 and thereafter remain constant. Demand is satisfied at the country level by either domestic production or imports, the balance between which is determined using a least-cost optimization considering commodity prices as well as the cost of fertilizer, irrigation water, and land conversion. A more detailed explanation of PLUM can be found in Alexander et al. (2018).

2.3 Simulation details

115 After a spinup of 500 years to bring vegetation and soil pools to a realistic starting point, a historical run spanning 1850 to 2005 was performed in LPJ-GUESS. The model state at the end of this run was used as the starting point for runs generating potential yields under different Representative Concentration Pathway (RCP) scenarios of climate and atmospheric CO₂ (van Vuuren et al., 2011). In each scenario, every grid cell is planted with each crop type, each of which is given six different management treatments in a factorial setup: fertilization of 0, 200, and 1000 kgN ha⁻¹ and either no irrigation or maximum irrigation. PLUM 120 then uses these potential yield estimates to generate time series of land use and management that satisfy crop and livestock demand calculated based on socioeconomic projections from the SSPs. Each socioeconomic scenario (SSP) is paired with a



climate scenario (RCP) based on what sort of climate change could be expected under each SSP's storyline: SSP1 uses RCP4.5, SSPs 3 and 4 use RCP6.0, and SSP5 uses RCP8.5. More details on the setup of the calibration and yield-generating runs can be found in the Supplementary Methods (Sect. SM1).

125 PLUM has been found to perform well in this coupled system; its recreation of historical patterns and projections into the future are discussed in Alexander et al. (2018). Here, after extending the historical run to 2010, we feed PLUM's projections of 2011–2100 land use, nitrogen fertilizer application, and irrigation intensity back into LPJ-GUESS to simulate their impacts over that period. We refer to these experiments as the “PLUM-forced” runs. The Supplementary Methods include a figure illustrating the overall workflow (Fig. SM1) and table summarizing a summary of the run types can be found in Table SM1.

130 In addition to PLUM-forced runs with time-varying future climate and atmospheric CO₂, we perform several experiments to examine the impact of different factors on the land-use and -management projections generated by PLUM and thus the ecosystem service indicators simulated by LPJ-GUESS in the PLUM-forced runs. By holding either climate, atmospheric CO₂, or land use and management constant over 2011–2100, we can estimate the contribution of each to changing ecosystem service indicators in the future. The indirect contributions of changing climate and atmospheric CO₂—i.e., how they affect the
135 land use and management pathways chosen by PLUM—are not considered.

2.3.1 Input data: LPJ-GUESS

Here, we describe the climate and land use data used in LPJ-GUESS. A summary can be found in the Supplementary Methods, Tables SM2–SM5.

The calibration run was forced with climate data from CRU-NCEP version 7 (Le Quéré et al., 2016), but with CRU TS3.24
140 precipitation (Harris et al., 2014) due to problems discovered in the CRU-NCEP precipitation data. All other runs used the atmospheric CO₂ concentrations and climate forcings from the Fifth Coupled Model Intercomparison Project (CMIP5; Taylor et al., 2012): specifically, the IPSL-CM5A-MR forcings (Dufresne et al., 2013), which were bias-corrected (Ahlström et al., 2012) to the 1961–1990 observation-based climate used by the calibration runs. Because not all SSP-RCP combinations are equally plausible, the PLUM-forced runs used future climate forcings corresponding to the most likely RCP for each SSP,
145 based on the SSP-RCP probability matrix from Engström et al. (2016a): i.e., RCP4.5 for SSP1, RCP6.0 for SSP3 and SSP4, and RCP8.5 for SSP5. Three instances of the yield-generating runs were performed: one with each of the RCP climate scenarios.

Time-evolving historical land use fractions—i.e., the fractions of land in each gridcell that are natural vegetation, cropland, pasture, or barren—were taken from the Land Use Harmonization v2 dataset (LUH2; Hurtt et al., in prep.). The MIRCA2000
dataset (Portmann et al., 2010) provided crop type distributions for the year 2000, which were used for all historical years.
150 Some mapping between MIRCA, LPJ-GUESS, and PLUM crop types was required, details of which can be found in the Supplementary Methods (Sect. SM2). Fertilizer application for the calibration run was taken from the dataset prepared for the Global Gridded Crop Model Intercomparison exercise (Elliott et al., 2015) of the Agricultural Model Intercomparison Project (AgMIP; Rosenzweig et al., 2013). In the historical period of other runs, nitrogen fertilizer application rates were taken from LUH2 (Hurtt et al., in prep). Manure N was added in the historical period according to the annually-varying maps given in



155 Zhang et al. (2017) held constant at year 2000 levels in the calibration run to match the use of the AgMIP fertilizer data. Simulation years outside the dataset's 1860–2014 range used 1860 and 2014 values, respectively.

The PLUM outputs at the beginning of the future period do not exactly match the land use and management forcings used at the end of the historical period. Feeding the PLUM outputs directly into LPJ-GUESS—causing large areas of agricultural abandonment and expansion between 2010 and 2011—would thus complicate interpretation of the results, especially of carbon cycling. We developed a harmonization routine based on that published for LUH1 (Hurt et al., 2011, <http://luh.umd.edu/code.shtml>). Briefly, the code begins with land use from LUH2 in 2010, then attempts to apply changes in land use area between PLUM's 2010 and 2011 outputs. In gridcells with no space to apply those changes, the algorithm attempts to find space in neighboring gridcells, expanding the search radius until the changes are satisfied. This process is then repeated, with the PLUM changes for 2011–2012 being applied to the harmonized 2011 land use map, and so on. More details on the harmonization procedure can be found in the Readme of the harmonization code (see Code Availability).

2.3.2 Input data: PLUM

In addition to the potential yields generated by LPJ-GUESS, PLUM considers a number of socioeconomic factors in estimating both future demand for commodities as well as how best to satisfy that demand. The Shared Socioeconomic Pathways (SSPs) provide a framework for generating scenarios of those socioeconomic factors' future evolution (O'Neill et al., 2014, 2015). Four of the five SSPs are used here. SSP1 characterizes a world shifting to a more sustainable pathway, with low population growth and strong technological and economic developments. SSP3 describes a pathway with strong population growth and intensive resource usage, low technological development and lessening globalization. SSP4 is a pathway of inequality with the potential for competition over resources and resource intensification. SSP5 is a pathway dependent on fossil fuels with low population growth, high economic and technological growth with strong globalization. (SSP2, a “middle of the road” pathway intermediate between the other four SSPs, is not considered here.) Scenario data on population (Jones and O'Neill, 2016) and GDP (Dellink et al., 2017) per country through 2100 were from version 0.93 of the SSP database (IIASA, 2014).

In addition to the input data provided by the SSPs, and following the approach described in Alexander et al. (2018), PLUM parameters—such as input and transport costs, tariffs, and minimum non-agricultural area—were also affected by the SSP narratives. Values were estimated for each SSP based on an interpretation of the storylines (O'Neill et al., 2015; Engström et al., 2016a) and can be found in Table SM6.

2.3.3 Experimental setups

In addition to the LPJ-GUESS runs forced with PLUM-output land use and management trajectories (harmonized as described in Sect. 2.3.1), six experimental runs were performed for each scenario, to disentangle the direct effects of climate change (including CO₂ concentration increases) from those of land use and management change. A “constant-climate+CO₂” 2011–2100 run used repeating 1981–2010 climate and constant 2010 CO₂ concentration; separate “constant-climate” and “constant-CO₂” runs were also performed. A “constant-LU” run used constant 2010 land use maps and management inputs. Finally, “onlyCO₂” and “onlyClimate” runs were performed using constant land use and either CO₂ concentrations or climate forcings



from the RCP scenarios. The results of these experimental runs were used to inform interpretation of the results but are mostly not presented here. The Supplementary Results file contains figures (numbers prefixed with SR) supporting claims derived from the experimental runs, in addition to other figures that were not included here to conserve space.

3 Results and Discussion

3.1 Land use areas and management inputs

LandSyMM simulates net global loss of natural land area over the 21st century in all scenarios (Fig. 1), with SSP3 seeing the greatest loss of area (10%), SSP1 seeing the least (3%), and SSPs 4 and 5 seeing an intermediate loss (6%). These patterns are mostly reversed for pasture area change, in which all scenarios see an increase, although the trajectory for SSP5 is more similar to that of SSP3. PLUM also simulates net increased cropland area globally in all scenarios, with SSPs 1 and 5 seeing the least increase, SSP4 seeing more, and SSP3 seeing the most.

Cropland expansion happens at a more or less constant rate in SSP3 and SSP4, but these scenarios experience very different trajectories of crop commodity demand: SSP4 approximately levels off around midcentury, whereas SSP3 experiences only a brief slowdown in growth followed by constantly increasing demand through 2100 (Fig. SR1). The majority of the increased demand in the first half of the century is satisfied by fertilizer application, which increases by more than 75% from the 2010s to the 2050s while crop area increases by less than 15%. However, management inputs per hectare in SSP3-60 approximately plateau after midcentury (Fig. SR2), while crop demand rises 16%. Cropland area expands about 10% between 2050, with boosted productivity—thanks to climate change and/or CO₂ fertilization—helping to satisfy the rest of the increased demand. Since SSP4-60 experiences the same climate and CO₂ fertilization but with level crop demand during the second half of the century, management inputs decrease after about 2050.

Although population growth in SSP5-85 is more than twice that of SSP1-45, PLUM simulates very similar trajectories of global crop demand in both: an increase until about 2040 followed by a decrease for the rest of the century, with SSP5-85 crop demand ending slightly higher. SSP5-85 livestock demand increases about 20% more than in SSP1-45, which explains the rest of the difference in global caloric needs between the two scenarios (Fig. SR1). However, because SSP5-85 experiences much stronger climate change and CO₂ increase, the two scenarios differ importantly in how they satisfy their crop demand over the century. Whereas cropland area increases more or less constantly in SSP1-45 (slightly slowing throughout), in SSP5-85 it decreases over the first two or so decades, increases slowly after about 2050, and ends at a slightly lower global extent than in SSP1-45 despite a jump in the early 2090s as feed becomes more important in raising ruminant livestock (Fig. SR3). Crop production remains similar between the two scenarios, especially in the first half of the century, because SSP5-85 applies much more fertilizer and irrigation water per hectare (Fig. SR2). This gap in these inputs narrows in the second half of the century as climate change and the CO₂ fertilization effect become even stronger in SSP5-85 relative to SSP1-45, although the latter also begins to increase what PLUM calls “other management” intensity (representing, e.g., pesticide application).

Several regional patterns in crop area stand out:

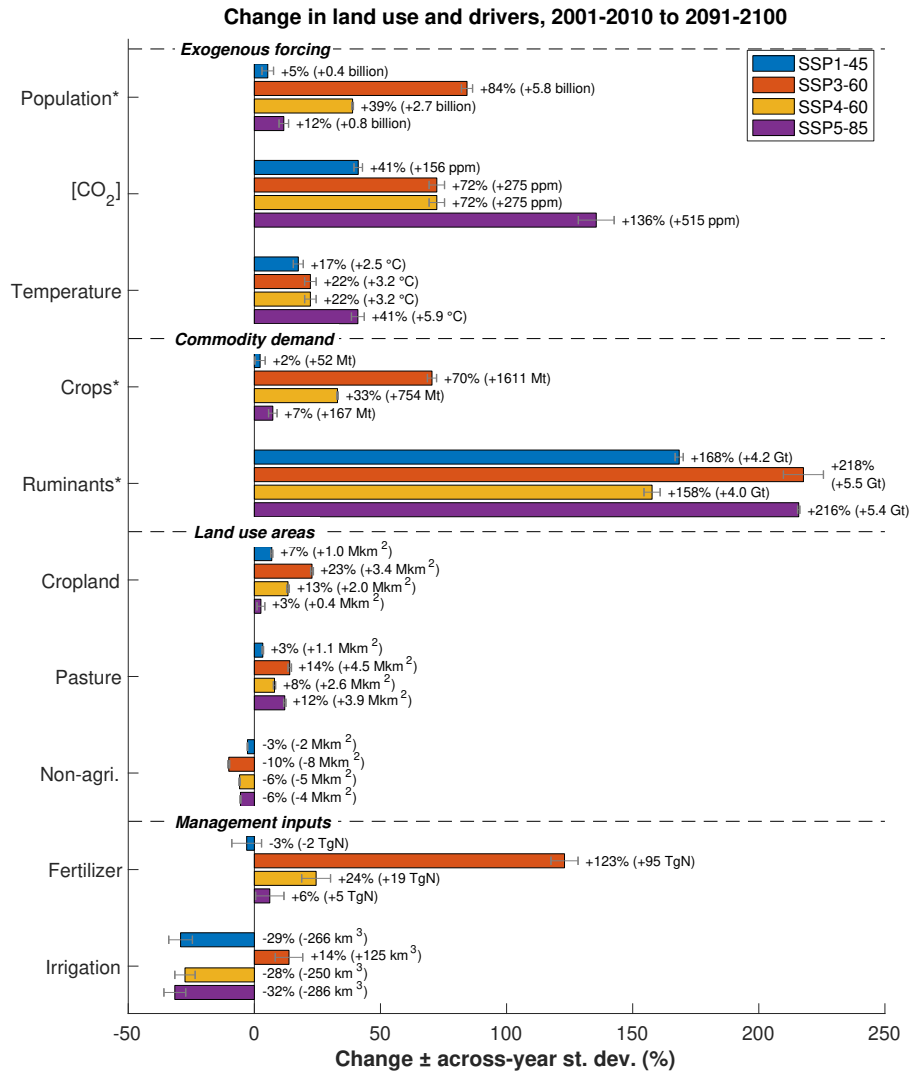


Figure 1. Percent change in global socioeconomic, land management, and atmospheric variables between 2001–2010 and 2091–2100. Whiskers represent interannual variability as standard deviation of the difference (i.e., $\sqrt{\sigma_{2001-2010}^2 + \sigma_{2091-2100}^2}$). Ruminant demand given in units of feed-equivalent weight. *Asterisk indicates variables whose baseline is 2010 instead of 2001–2010 mean.

220 – North America loses cropland in parts of the Great Plains (mainly C₃ cereals; Fig. SR4) and the Midwestern U.S. (mainly
 oilcrops; Fig. SR5) in all scenarios. This is at least partially replaced—to a varying extent among the scenarios—with
 land in Alaska and the southeastern U.S. In the latter, new cropland is mostly planted with energy crops (SSP3-60 and
 SSP4-60; Fig. SR6) and rice (SSP3-60; Fig. SR7). New cropland in Alaska is entirely planted with spring wheat and is
 most extensive in SSP5-85 (Fig. SR4), which sees the largest increase in North American cereal demand—nearly 250%
 225 by the end of the century (Fig. SR8)—but also the largest potential yield increase in Alaska, thanks to RCP8.5’s high

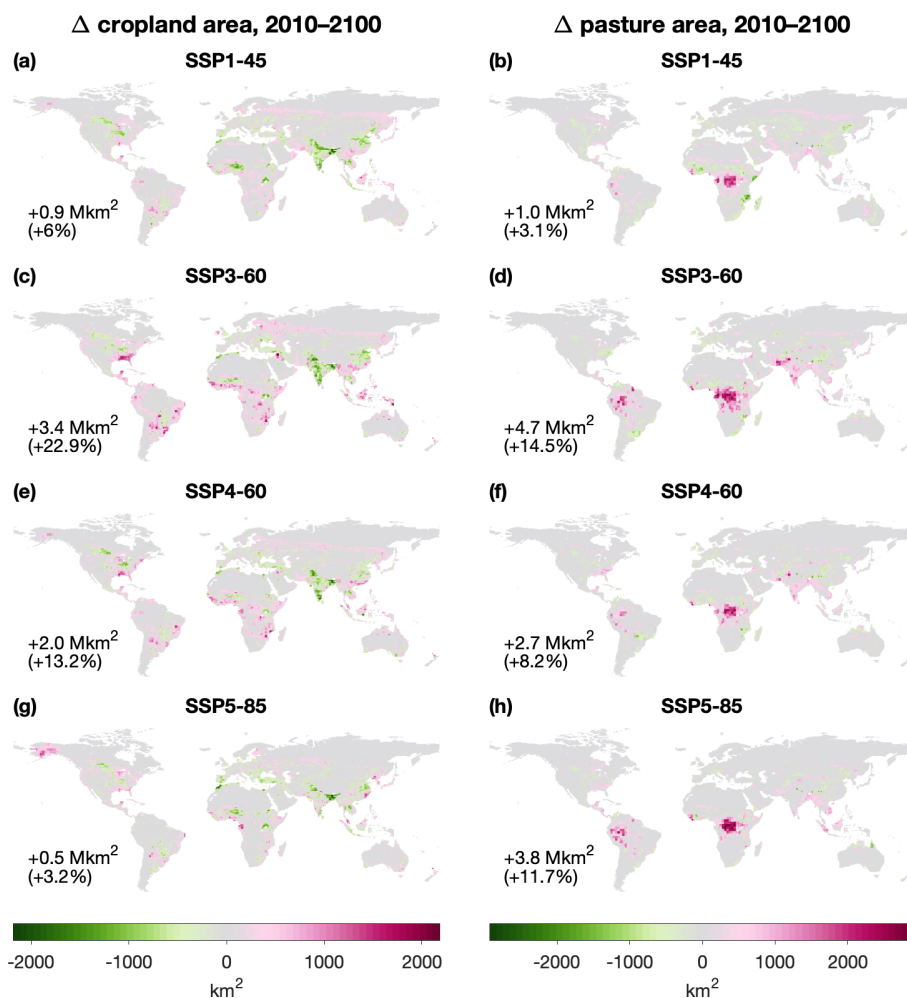


Figure 2. (Left column) Change in cropland area from 2010 (LUH2) to 2100 (harmonized PLUM) under each SSP-RCP scenario. **(Right column)** As left column, but for pasture. Note that color scales differ between columns.

warming and CO₂ fertilization. Indeed, by 2091–2100, the potential yield of rainfed C₃ cereals there is similar to or exceeds that of the parts of the Great Plains where cropland is lost (Fig. SR9).

- 230
- Although crop demand in South Asia increases by more than 100% in SSP5-85 and 170% in SSP3-60 (Fig. SR10), that region loses large amounts of cropland. Imports increase from zero to 5–30% of South Asia’s food and feed crop demand (respectively) by the end of the century, but to satisfy the remaining 70–95%, PLUM calculates that the region’s crop production would approximately double in both scenarios (Fig. SR11). While some of this is accomplished through increased management inputs in a region where the yield gap is large in the baseline, it also depends markedly on yield boosts due to climate change and rising CO₂ concentrations: C₃ cereal yields in the constant land-use experiments triple



235 (RCP 6.0) or quadruple (RCP 8.5) across large parts of Pakistan and India. This is mostly due to a CO₂ fertilization effect, especially in RCP 8.5, which sees widespread areas of yield decline in the onlyClimate experiment (Fig. SR12).

– Sub-Saharan Africa sees even larger crop production increases, ranging from +200% in SSP1-45 to +500% in SSP3-60 (Fig. SR13). In contrast to South Asia, nearly the entire region experiences negative yield effects from the changing climate, and the counteracting effect of CO₂ fertilization results in yields that are only net slightly boosted in the constant-LU experiments (e.g., Fig. SR12). The heightened production comes instead from increased management inputs and, to
240 a much smaller degree, cropland expansion.

Pasture is projected to expand significantly in the western Amazon in SSP3-60 and SSP5-85, and even more so in all scenarios in the African rainforest (Fig. 2). This tropical deforestation is largely driven by the increasing consumption of ruminant products in those regions: As incomes increase in developing tropical countries, PLUM forecasts greater consumption of commodities such as meat and milk and a reduction in staples such as starchy roots and pulses (Keyzer et al., 2005; Tilman
245 et al., 2011). Depending on the SSP, ruminant products are simulated to account for 23–43% of calories in central Africa by 2100, compared to only 4–7% of calories consumed in 2010 (caloric density derived from FAOSTAT, 2018c). Between 50 and 98% of the ruminant production increase in central Africa goes to this domestic consumption.

The African pasture expansion even occurs in SSP1-45, the “Sustainability” scenario (O’Neill et al., 2015), in which LandSyMM simulates a net global pasture expansion of about 1 Mkm². For comparison, five other land use models all saw
250 SSP1 pasture area decrease, by an average of about 3.4 Mkm² (Popp et al., 2017). Some of the discrepancy between the LandSyMM land-use trajectories and those of the other models is likely due to inherent differences in how processes are represented. Several factors related to experimental setup and overall model structure may contribute as well.

First, PLUM makes no assumption about changes in food production needs besides what occurs due to population and GDP changes. The storyline for SSP1, however, with its “low challenges to mitigation,” suggests that people will gradually shift to
255 lower-meat diets (O’Neill et al., 2015) than would be expected given GDP levels, at first at least in high-income countries. IMAGE—which simulates a decrease in pasture area of about 7 Mkm² by the end of the century (Doelman et al., 2018)—incorporates this dietary shift as a 30% (global) reduction in meat consumption relative to what would have otherwise been simulated, and additionally includes a 33% reduction in food supply chain losses to represent efficiencies from improved management and infrastructure (Doelman et al., 2018). Weindl et al. (2017) use the MAgPIE model to show that, under a
260 scenario like ours where historical differences in livestock production efficiency are maintained or exacerbated, a shift to lower-meat diets can reduce the expansion of pasture in sub-Saharan Africa by over 50%.

Second, the land-use modeling components of most integrated assessment models (IAMs)—for example, all those contributing to the LUH2 trajectories (Hurtt et al., 2011)—include demand for timber and other products. The carbon value of forests (and land more generally) can also be included by some, even if forest products are not explicitly modeled (e.g., MAg-
265 PIE; Humpenöder et al., 2014), which could come into play in scenarios with policy-based incentives designed to minimize emissions from deforestation and degradation and/or to maximize carbon sequestration. In contrast, PLUM includes neither forest products nor land carbon value. The only “friction” PLUM considers in converting a forest to agriculture is the cost



of conversion, with the opportunity cost of lost forest products or services ignored. Similarly, the only incentive to replace existing agricultural land with forest would be to avoid costs associated with production. Work currently underway to include forest products, payments for carbon sequestration, and managed forestry into LandSyMM may result in more forest simulated over the course of the century. This is especially likely for SSP1, whose storyline specifies a gradual improvement in how the global commons are managed (O'Neill et al., 2015). As an example, IMAGE represented this improvement in SSP1-45 by (a) disallowing clearing of forests with carbon density greater than 200 tons ha⁻¹ and (b) reforesting half of the world's degraded or former forest.

The difference in land-use area between the most extreme scenarios is much higher in this work than in Alexander et al. (2018), by around 500% for cropland and 700% for pasture. The primary reason for this increase in inter-scenario variation is that Alexander et al. (2018) used the SSP2 socioeconomic scenario for all RCPs, whereas here we compare different SSPs paired with appropriate RCPs. Even with this increased spread, however, the LandSyMM trajectories are more closely clustered than those from some other land use models. IMAGE, for example, projects a range of cropland area increase from 0.4 Mkm² to 5.3 Mkm² across the five SSPs, and pasture trajectories ranging from a decrease of 7.3 Mkm² to an increase of 4.4 Mkm² (Doelman et al., 2018). As described above, IMAGE makes a number of assumptions (based on the SSP storylines) regarding future deviations from historical "business-as-usual" trends and relationships, including dietary shifts, infrastructure efficiency improvements, and forest conservation.

3.2 Ecosystem service indicators

3.2.1 Carbon storage

Carbon stored in the land system increases for all SSP-RCP scenarios, primarily due to an increase in vegetation carbon (Fig. 3). The increase in each scenario relative to the others depends on both intensity of climate change as well as amount of natural land lost. The large increase of atmospheric CO₂ (and thus greater carbon fertilization) in RCP 8.5 compared to RCP 6.0 means that SSP5-85 has a much greater increase in terrestrial carbon storage than SSP4-60, despite those scenarios having similar trajectories of natural land area (Fig. 1). SSP3-60, which had the most natural land lost but only intermediate carbon fertilization, sees the lowest increase in terrestrial C storage over the century—less than a third that of SSP4-60, which has the same trajectory of changing climate and atmospheric CO₂ concentration but a much smaller population increase.

The contrast between effects of changing climate and atmospheric CO₂ concentration vs. changing land use and management is starker for vegetation carbon than any other indicator variable examined here. In the constant-LU experiment, vegetation carbon increased 35%, 43%, 43%, and 54% for SSP1-45, SSP3-60, SSP4-60, and SSP5-85, respectively. The constant-climate+CO₂ experiment, on the other hand, saw respective *decreases* of 5%, 15%, 8%, and 9%.

Vegetation carbon increases are most pronounced in the tropical and boreal forests (Fig. 4) and are due primarily to CO₂ fertilization, although increasing temperatures and growing season length also contribute in the boreal zone (Fig. SR14). Extensive conversion to pasture far outweighs any carbon fertilization effect in the African tropical forest, which loses nearly all of its vegetation carbon and up to half its total carbon by 2100 in all scenarios.

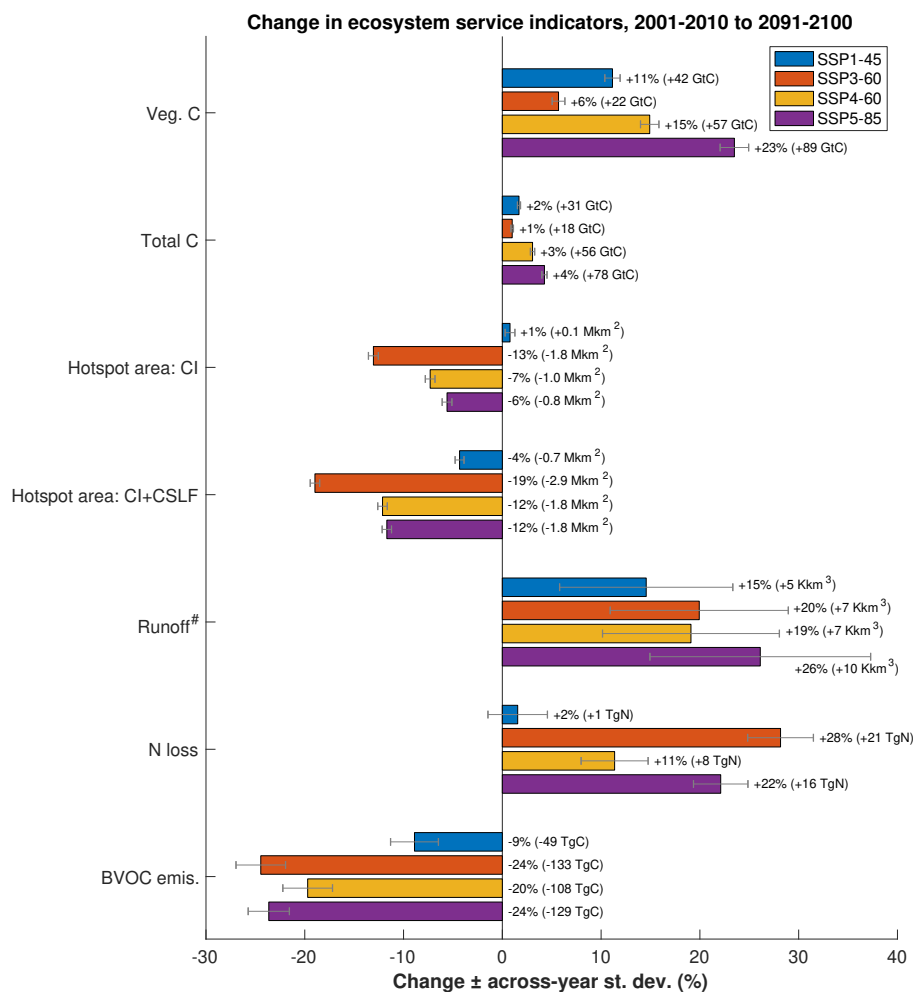


Figure 3. Percent global change in ecosystem service indicators between 2001–2010 and 2091–2100. Whiskers represent standard deviation of the difference (i.e., $\sqrt{\sigma_{2001-2010}^2 + \sigma_{2091-2100}^2}$). CSLF: Congolian swamp and lowland forests (see Sect. 3.2.5). [#]The time periods compared for runoff were 1971–2000 and 2071–2100 due to high interannual variability.

Our results for carbon sequestration fall near the lower end of previously-reported projections. Brovkin et al. (2013) examined the change in land carbon storage over 2006–2100 for a number of climate and land surface models. They found that the IPSL-CM5A-LR Earth system model, when forced with emissions and land use change from RCP8.5, simulated uptake of ~400 GtC. This is much greater than our finding of ~78 GtC under SSP5-85 (Fig. 4) despite their land use change scenario (from LUH1; Hurtt et al., 2011) having lost about 30% more non-agricultural land. The difference is probably due in large part to our pasture expansion in the central African and western Amazon rainforests (and to a lesser extent, cropland expansion in Alaska). Most of their agricultural expansion occurs in the northern sub-Saharan African savannas, and even there the change (in units of percentage of the grid cell) only reaches about 30%. Moreover, none of the models in Brovkin et al. (2013) limit

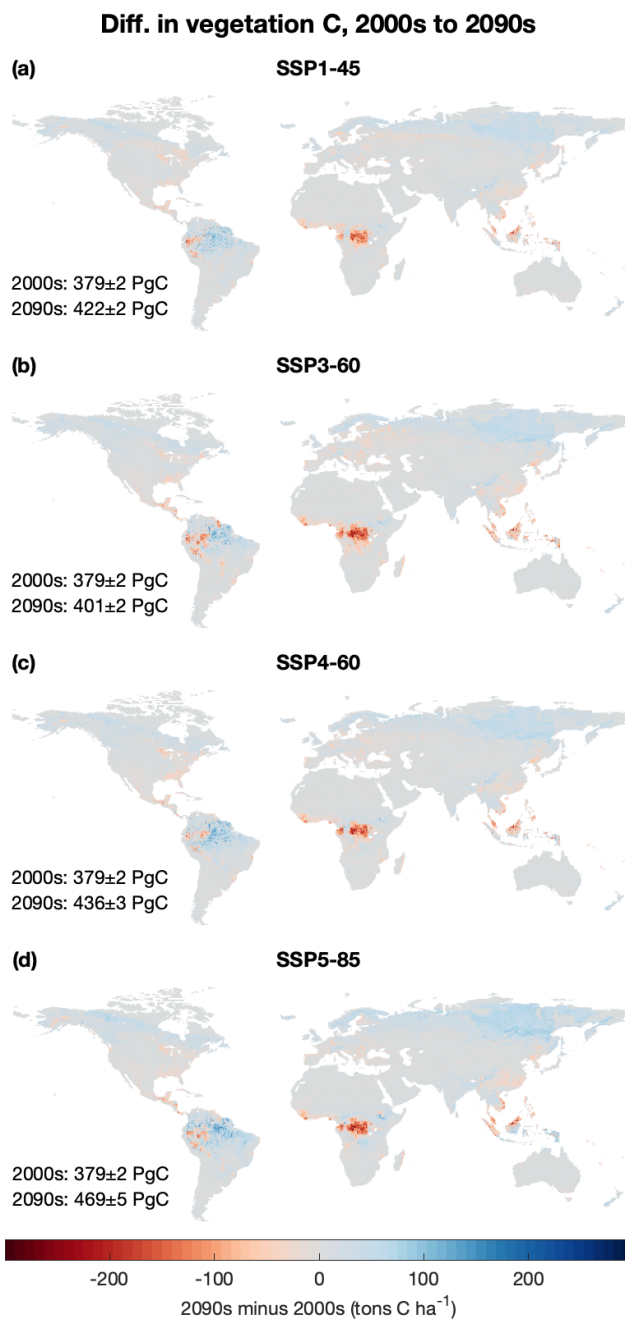


Figure 4. Maps showing difference in mean vegetation carbon between 2001–2010 (“2000s”) and 2091–2100 (“2090s”) for (a) SSP1-45, (b) SSP3-60, (c) SSP4-60, (d) SSP5-85. Overlaid text provides decadal means and standard deviations.

310 photosynthesis based on nitrogen availability. However, we also see low simulated carbon sequestration under constant land use compared to the models in Nishina et al. (2015), even when excluding models that did not simulate nitrogen limitation.



Another study with LPJ-GUESS, Krause et al. (2017), used land use trajectories from the IMAGE and MAgPIE IAMs given RCP2.6 and SSP2, finding an increase in total land carbon pools of 34 GtC and 64 GtC, respectively. Land use scenario played an important role in those results and likely contributes to the discrepancy with ours: Their IMAGE pasture area increased from ~35 Mkm² to ~40 Mkm², whereas their MAgPIE pasture area decreased to ~30 Mkm² and our SSP1-45 pasture stays
315 around ~32 Mkm². The IMAGE cropland area used in the baseline run of Krause et al. (2017) stayed approximately constant at ~18 Mkm², as does our SSP1-45's (although at ~15 Mkm²), but their MAgPIE cropland area increased to ~20 Mkm². Other important differences between the runs in Krause et al. (2017) and ours include our use of different climate forcings and associated photosynthesis scaling parameters.

3.2.2 Runoff

320 Global runoff increases in all scenarios (Fig. 5). Again, SSP3 and SSP4 (the two RCP6.0 scenarios) see similar changes; SSP1-45 sees a smaller increase, and SSP5-85 sees the greatest. Comparison of the experimental runs shows that climate change is the most important factor in this increase at a global level in all scenarios (Fig. SR15). Increasing CO₂ levels generally tend to decrease runoff, a result also seen in two global vegetation models analyzed by Davie et al. (2013), although two others in that comparison showed the opposite effect. Land-use change makes the least difference in terms of global annual runoff, but can
325 be important at the regional level. Deforestation in central Africa, for example, is the primary driver of increasing mean annual runoff there.

Such regional patterns in runoff change are arguably more important than global means, since impacts of low water and flooding are actually felt at the level of individual river basins. Between 1971–2000 and 2071–2100 under SSP5-85, 44% of land area saw increasing flood risk, with a mean P95_{month} increase of 48%. Drought risk increased in 34% of land area, which
330 saw a mean P5_{year} decrease of 59%. At the same time, however, 43% of gridcells saw decreasing flood risk (mean P95_{month} decrease 50%), and 44% saw decreasing drought risk (mean P5_{year} increase 88%). Other scenarios saw similar fractions of area affected, but smaller mean magnitude of change in flood or drought metric.

Most of the changes in SSP5-85 result from climate change, with some notable exceptions. Land-use change alone contributes notably to increasing drought risk in Iraq, Pakistan, India's Punjab province, the Great Plains of the U.S., and eastern
335 China (Fig. 5); it contributes to increasing flood risk in northeastern China, India's Rajasthan province, and the central African rainforest. Land-use change can also serve to counteract the impacts of climate change on runoff. For example, the severity of very low runoff events increases in central America, but it would have increased more if not for the expansion of agriculture there. The effects of land-use change on runoff might be stronger and more widespread if LPJ-GUESS were run coupled with a climate model, which would account for associated changes in land-atmosphere water and energy fluxes that can have similar
340 impacts on the hydrological cycle as greenhouse gas emissions (Quesada et al., 2017).

The LandSyMM results for SSP5-85 are compared with the RCP8.5 ensemble from Asadieh and Krakauer (2017) in Table 1. Our results for fraction of land in each class are roughly similar for most classes, except for increasing drought risk, more of which is found in the Asadieh and Krakauer (2017) ensemble. In all categories, LandSyMM finds a mean effect of stronger magnitude. Some differences between our results and those of Asadieh and Krakauer (2017) might be expected because we

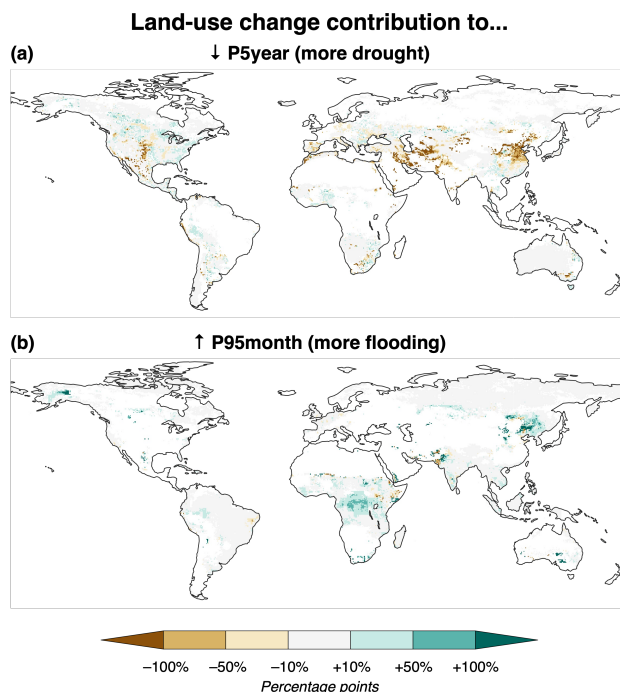


Figure 5. Contribution of land-use change in SSP5-85 to (a) decreasing P5_{year} (drought) and (b) increasing P95_{month} (flooding) between 1971–2000 and 2071–2100. White areas either did not have decreasing P5_{year} or increasing P95_{month}, respectively, or were excluded due to low baseline runoff (after Asadieh and Krakauer, 2017). Contribution calculated as difference between full run and constant-LU run.

345 used a single climate model and monthly instead of daily values for P95. Perhaps more importantly, however, LPJ-GUESS is not a full hydrological model: e.g., it does not include river routing. The effect of this can be somewhat explored by aggregating our results to the basin scale, at which LPJ has been shown to compare well to dedicated hydrological models (Gerten et al., 2004). Aggregating to the basins with which PLUM determines irrigation water availability does not change the fraction of included land area in any class by more than two percentage points, except for decreasing drought risk, which goes from 49% to 58% of included land. The mean change within every class is reduced in absolute terms, bringing our results closer to those from Asadieh and Krakauer (2017).

350

3.2.3 Nitrogen losses

While the evolution of total global nitrogen loss is fairly similar for all scenarios over the first two decades of the simulation, there are notable differences by the end of the century. N loss showed little net change over the century in SSP1-45, whereas SSP3-60 saw a large increase in total N losses. SSP4-60 did not see a notable change in total N losses. SSP5-85 saw an increase in total N losses, although less than that of SSP3-60.

355



Table 1. Fraction of included land in each group of changing drought and flood risk. Numbers in parentheses give each group's mean percent change. Increasing and decreasing drought risks correspond respectively to decreasing and increasing P5; increasing and decreasing flood risks correspond respectively to increasing and decreasing P95. AK2017: Asadieh and Krakauer (2017).

Class	By gridcell	By basin	AK2017
↑ drought risk	38% (-59%)	39% (-58%)	57% (-51%)
↓ drought risk	49% (+88%)	58% (+49%)	43% (+30%)
↑ flood risk	49% (+48%)	51% (+32%)	48% (+25%)
↓ flood risk	47% (-50%)	46% (-42%)	52% (-21%)

Our N loss at the end of the historical period was similar to that of Krause et al. (2017), but whereas their runs estimated an increase in N losses of 60–80% under RCP2.6, ours under SSP1-45 increased only 2%. Krause et al. (2017) used fertilizer information from IMAGE and MAgPIE, which they note often exceeded what plants in LPJ-GUESS could actually take up.
360 Coupling LPJ-GUESS with PLUM provides for a more internally consistent estimate of future N losses.

One interesting pattern is that climate and management changes can have similar effects on N losses. SSP3-60 sees global fertilizer application more than double by the end of the century, while SSP5-85 fertilizer application at end of the run is slightly lower than in 2011 (Fig. 1). This is reflected in the N losses for the constant-climate+CO₂ experiment, which increase 25% by the 2090s in SSP3-60 but only 7% in SSP5-85. However, in the full run, SSP3-60's N losses increase only about 27%
365 more than SSP5-85's (Fig. 3). This is because the latter experiences higher average global temperatures (increasing gaseous losses) and a greater increase in runoff (increasing dissolved losses), due to the extreme RCP8.5 climate change scenario; in the constant-LU experiment, N losses in SSP3-60 and SSP5-85 increase by 15% and 24%, respectively. In either case—but especially under SSP3-60—these increases in fertilizer usage and concomitant nitrogen pollution would exacerbate humanity's already unsustainable impacts on nutrient cycling (Rockström et al., 2009).

370 3.2.4 BVOCs

Global combined BVOC emissions over 2001–2010 totaled ~546 TgC yr⁻¹ (~503 and ~43 TgC yr⁻¹ for isoprene and monoterpenes, respectively), which compares well with estimates from LPJ-GUESS (without PLUM) and other models (Arneth et al., 2008; Hantson et al., 2017; Szogs et al., 2017). Emissions decline in all scenarios: by the most in SSP3-60 and SSP5-85, slightly less in SSP4-60, and the least in SSP1-45 (Fig. 3). This reflects a combination of the effects of land-use change and
375 [CO₂] increases. In the “constant-climate+CO₂” experiment, declines in combined BVOC emissions closely reflect declines in non-agricultural land area (most decrease in SSP3-60, less in SSP4-60 and SSP5-85, and least in SSP1-45; Fig. SR16). This is a function of the much higher BVOC emissions potential of forests relative to cropland and pasture, as also seen in results from Hantson et al. (2017) and Szogs et al. (2017). In the full experiment, BVOC emissions decline more in SSP5-85 than in SSP4-60 because the former has higher atmospheric [CO₂], which suppresses BVOC formation.



380 Decreases in isoprene emissions are primarily driven by tropical deforestation for agriculture, especially the expansion of
pasture in central Africa and South America, and to a lesser extent by the expansion of cropland for bioenergy in the south-
eastern U.S (Fig. SR17). The suppressive effect of increasing $[\text{CO}_2]$ is mostly counteracted in all RCPs by rising temperatures,
which increase BVOC volatility. Monoterpene emissions in what is now tundra increase as woody vegetation expands there,
but present-day boreal forests are the main drivers of declining monoterpene emissions. This is primarily due to the BVOC-
385 suppressing effect of increasing $[\text{CO}_2]$, but land-use change also contributes, especially in Alaska (Fig. SR18).

The globally decreased BVOC emissions in all scenarios could contribute a cooling effect in the future, due to expected lower
tropospheric ozone concentrations, shorter methane lifetime, and enhanced photosynthesis thanks to more diffuse radiation.
This would be counteracted somewhat by warming arising from the reduced formation of secondary aerosols, and it is important
to note that the effects on climate are likely to vary from region to region (Rosenkranz et al., 2014). Southeast Asia and the
390 southeastern U.S. are populous areas that could see public health benefits from the deforestation-induced reduction of isoprene
emissions and associated ozone levels. However, note that in the latter (and to a lesser extent the former), agricultural expansion
is mainly for growing bioenergy crops simulated in LPJ-GUESS as Miscanthus; BVOC levels would be reduced much less (or
perhaps even increased) if woody bioenergy crops were grown instead on the same area (Rosenkranz et al., 2014). Moreover,
the loss of natural land is itself associated with myriad negative health impacts (Myers et al., 2013), so it would be shortsighted
395 to view deforestation-induced BVOC reductions as a public health boon.

It is important to keep in mind that the implications of changing BVOC emissions depend on complex, regionally-varying
atmospheric chemistry that governs their effects on existing species (e.g., methane) and the formation of secondary products
(e.g., ozone and aerosols). The LandSyMM framework, lacking as it does an atmospheric chemistry model, can thus inform
only a surface-level discussion of the possible effects of changing BVOCs.

400 3.2.5 Biodiversity hotspots

The large expansion of agricultural land in SSP3-60 has direct consequences for habitat in biodiversity hotspots, which lose
over 13% of their non-agricultural land in that scenario (Fig. 3). No other scenario lost more than 8%, and SSP1-45 actually
saw a slight gain. However, note that the central African rainforest is not included in the CI hotspots, since that region did not
meet the criterion regarding how much of its primary vegetation had been lost (Myers et al., 2000; Mittermeier et al., 2004).
405 The amount of deforestation projected there in all scenarios would undoubtedly result in great impacts to regional and global
biodiversity. We thus checked how much hotspot area is lost if we include the five ecoregions classified by Olson et al. (2001)
as Congolian swamp and lowland forests (CSLF), which together roughly correspond to the area of pasture expansion common
to all scenarios, into a new “CI+CSLF” hotspot map. This paints a worse picture in all scenarios, nearly doubling hotspot area
loss in SSP3-60, more than doubling it in SSP4-60 and SSP5-85, and changing the 1% gain of SSP1-45 to a 9% loss.

410 Previously, Jantz et al. (2015) performed a similar analysis using the same hotspots, but with the LUH1 land-use scenarios
over 2005–2100. Although they considered only primary land as habitat—i.e., any land that had once been agriculture or
experienced wood harvest was “uninhabitable”—their results can still provide a useful perspective. Jantz et al. (2015) found
losses of primary natural hotspot land of 25% in RCP4.5, 40% in RCP6.0, and 58% in RCP8.5. However, they found a smaller

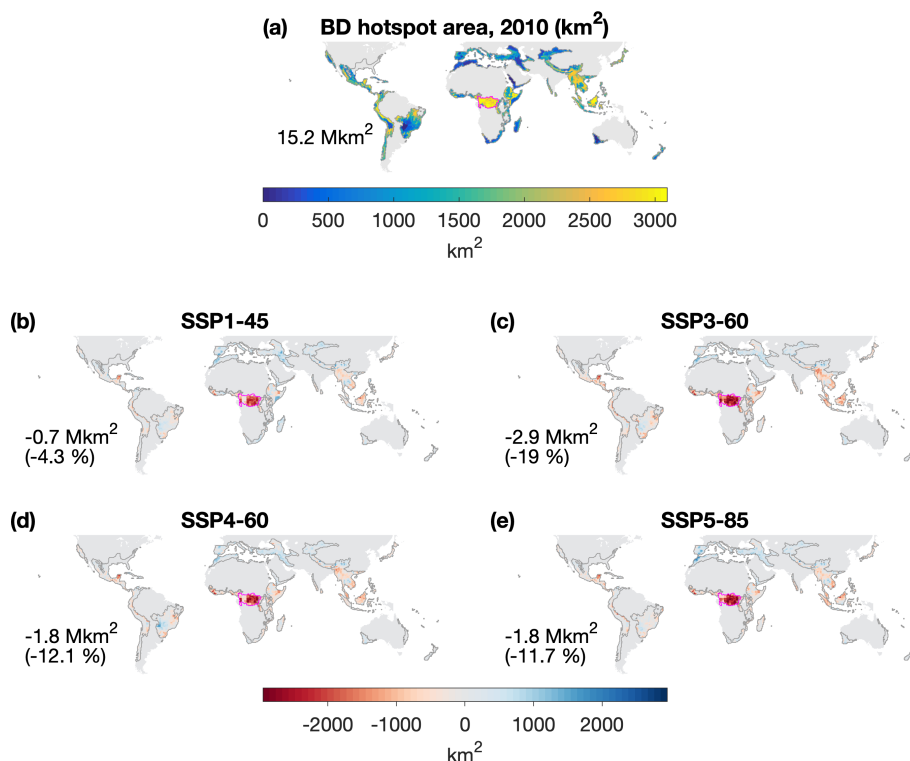


Figure 6. (a) Area (from LUH2) of non-agricultural land in “CI+CSLF” hotspots in 2010; (b–e) change in non-agricultural land area there by 2100 for each scenario. Black outlines indicate CI hotspots; magenta outline indicates CSLF region.

effect of land-use change using species-area curves to estimate the number of endemic species driven to extinction: 0.2–25%
415 between 2005 and 2100. This is in part due to the shape of the species-area curves used in their calculations, in which the
rate of extinctions per hectare lost is high at the beginning of land clearance in a region but falls as more area is cleared. This
nonlinear effect is important to consider, especially considering how much land has (by definition) been cleared already in the
hotspots, but such an analysis is beyond the scope of the present study.

Hof et al. (2018) considered the effects of both climate and land-use change under RCPs 2.6 and 6.0 on species distribution
420 models of amphibians, birds, and mammals. They found that the area of land impacted by these combined threats was ap-
proximately equal between the two scenarios for birds and mammals (with more area affected for amphibians under RCP6.0),
because although climate change was less detrimental under RCP2.6, to meet such an ambitious climate change target, that
scenario required more land devoted to growing bioenergy crops. We may see a similar effect between SSP4-60 and SSP5-85:
if ignoring cropland planted with *Miscanthus*, we see losses of natural land area in the CI+CSLF hotspots of approximately
425 1.1 and 1.5 Mkm², respectively, compared to about 1.8 Mkm² lost in both scenarios with *Miscanthus* cropland included. Ig-
noring *Miscanthus* cropland results in a CI+CSLF hotspot area net gain of <0.1 Mkm² for SSP1-45 and a loss of 2.0 Mkm² for
SSP3-60.



4 Conclusions

This work is among the first to consider the impacts of future land use and land management change on a suite of ecosystem
430 services under different scenarios of climate and socioeconomic change. We show that storylines with high socioeconomic
challenges to climate change mitigation—SSP3 and SSP5—consistently have some of the most severe consequences for the
natural world and the benefits it provides humanity via carbon sequestration, biodiversity, and water regulation. These two
scenarios also most strongly affect biogeochemical cycling of nitrogen and BVOCs; while increases in nitrogen losses are
generally detrimental, the impact of decreased BVOC emissions is likely to vary regionally.

435 Policymakers and other stakeholders need options for how we can meet the needs of a growing and changing society while
achieving climate and sustainable development goals (Benton et al., 2018). Some progress has already been made in this regard
at landscape and global scales (Eitelberg et al., 2016; Verhagen et al., 2018). LandSyMM, and analyses it enables such as the
ones presented here, can be another powerful tool in this aspect of the science-policy interface.

Code availability. The code for harmonizing land use and management is available for download on GitHub (Rabin, 2019).

440 *Author contributions.* All authors contributed to the conceptual design of LandSyMM. S. Rabin composed most of this manuscript, although
all authors contributed to its editing. S. Rabin performed most analyses, with R. Henry helping to interpret PLUM results. P. Alexander
and R. Henry managed PLUM code and performed PLUM runs. S. Rabin made changes as described to LPJ-GUESS code and performed
LPJ-GUESS runs.

Competing interests. The authors declare that they have no conflict of interest.

445 *Acknowledgements.* A.A. and S.R. acknowledge funding from the Helmholtz Association Impulse and Networking fund and the HGF ATMO
programme. P. Alexander and R.H. were supported by the UK's Global Food Security Programme project "Resilience of the UK food system
to Global Shocks" (RUGS, BB/N020707/1). In addition, the authors would like to thank Jonathan Doelman for sharing data about the IMAGE
scenarios (Doelman et al., 2018). This is paper number FILL ON ACCEPTANCE of the Birmingham Institute of Forest Research.



References

- 450 Ahlström, A., Schurgers, G., Arneth, A., and Smith, B.: Robustness and uncertainty in terrestrial ecosystem carbon response to CMIP5 climate change projections, *Environmental Research Letters*, 7, 044 008–10, <https://doi.org/10.1088/1748-9326/7/4/044008>, <http://iopscience.iop.org/article/10.1088/1748-9326/7/4/044008/meta>, 2012.
- Alexander, P., Rabin, S. S., Anthoni, P., Henry, R., Pugh, T. A. M., Rounsevell, M. D. A., and Arneth, A.: Adaptation of global land use and management intensity to changes in climate and atmospheric carbon dioxide, *Global Change Biology*, 24, 2791–2809, <https://doi.org/10.1111/gcb.14110>, <http://doi.wiley.com/10.1111/gcb.14110>, 2018.
- 455 Arneth, A., Niinemets, U., Pressley, S., Bäck, J., Hari, P., Karl, T., Noe, S., Prentice, I. C., Serça, D., Hickler, T., Wolf, A., and Smith, B.: Process-based estimates of terrestrial ecosystem isoprene emissions: incorporating the effects of a direct CO₂-isoprene interaction, *Atmospheric Chemistry and Physics*, 7, 31–53, <https://doi.org/10.5194/acp-7-31-2007>, <http://www.atmos-chem-phys.net/7/31/2007/>, 2007.
- Arneth, A., Monson, R. K., Schurgers, G., Niinemets, U., and Palmer, P. I.: Why are estimates of global terrestrial isoprene emissions so similar (and why is this not so for monoterpenes)?, *Atmospheric Chemistry and Physics*, 8, 4605–4620, <https://doi.org/10.5194/acp-8-4605-2008>, <http://www.atmos-chem-phys.net/8/4605/2008/>, 2008.
- 460 Asadieh, B. and Krakauer, N. Y.: Global change in streamflow extremes under climate change over the 21st century, *Hydrology and Earth System Sciences*, 21, 5863–5874, <https://doi.org/10.5194/hess-21-5863-2017>, <https://www.hydrol-earth-syst-sci.net/21/5863/2017/>, 2017.
- Ashmore, M. R.: Assessing the future global impacts of ozone on vegetation, *Plant, Cell and Environment*, 28, 949–964, <https://doi.org/10.1111/j.1365-3040.2005.01341.x>, <https://onlinelibrary.wiley.com/doi/full/10.1111/j.1365-3040.2005.01341.x>, 2005.
- 465 Benton, T. G., Bailey, R., Froggatt, A., King, R., Lee, B., and Wellesley, L.: Designing sustainable landuse in a 1.5°C world: the complexities of projecting multiple ecosystem services from land, *Current Opinion in Environmental Sustainability*, 31, 88–95, <https://doi.org/10.1016/j.cosust.2018.01.011>, <https://doi.org/10.1016/j.cosust.2018.01.011>, 2018.
- Brovkin, V., Boysen, L., Arora, V. K., Boisier, J. P., Cadule, P., Chini, L., Claussen, M., Friedlingstein, P., Gayler, V., van den Hurk, B. J. J. M., Hurtt, G. C., Jones, C. D., Kato, E., de Noblet-Ducoudré, N., Pacifico, F., Pongratz, J., and Weiss, M.: Effect of anthropogenic land-use and land-cover changes on climate and land carbon storage in CMIP5 projections for the twenty-first century, *Journal of Climate*, 26, 6859–6881, <https://doi.org/10.1175/JCLI-D-12-00623.1>, <http://journals.ametsoc.org/doi/abs/10.1175/JCLI-D-12-00623.1>, 2013.
- Castañeda-Álvarez, N. P., Khoury, C. K., Achicanoy, H. A., Bernau, V., Dempewolf, H., Eastwood, R. J., Guarino, L., Harker, R. H., Jarvis, A., Maxted, N., Müller, J. V., Ramirez-Villegas, J., Sosa, C. C., Struik, P. C., Vincent, H., and Toll, J.: Global conservation priorities for crop wild relatives, *Nature Plants*, pp. 1–6, <https://doi.org/10.1038/nplants.2016.22>, <http://dx.doi.org/10.1038/nplants.2016.22>, 2016.
- 475 Ciais, P., Sabine, C., Bala, G., Bopp, L., Brovkin, V., Canadell, J., Chhabra, A., DeFries, R., Galloway, J., Heimann, M., Jones, C., Le Quéré, C., Myneni, R., Piao, S., and Thornton, P.: 6: Carbon and Other Biogeochemical Cycles, in: *Climate Change 2013: The Physical Science Basis. Contribution of Working Group I to the Fifth Assessment Report of the Intergovernmental Panel on Climate Change*, edited by Stocker, T. F., Qin, D., Plattner, G.-K., Tignor, M., Allen, S. K., Boschung, J., Nauels, A., Xia, Y., Bex, V., and Midgley, P. M., Cambridge, United Kingdom and New York, NY, USA, 2013.
- 480 Davie, J. C. S., Falloon, P. D., Kahana, R., Dankers, R., Betts, R. A., Portmann, F. T., Wisser, D., Clark, D. B., Ito, A., Masaki, Y., Nishina, K., Fekete, B., Tessler, Z., Wada, Y., Liu, X., Tang, Q., Hagemann, S., Stacke, T., Pavlick, R., Schaphoff, S., Gosling, S. N., Franssen, W., and Arnell, N.: Comparing projections of future changes in runoff from hydrological and biome models in ISI-MIP, *Earth System Dynamics*, 4, 359–374, <https://doi.org/10.5194/esd-4-359-2013>, <https://www.earth-syst-dynam.net/4/359/2013/>, 2013.



- 485 Dellink, R., Chateau, J., Lanzi, E., and Magné, B.: Long-term economic growth projections in the Shared Socioeconomic Pathways, *Global Environmental Change-Human and Policy Dimensions*, 42, 200–214, <https://doi.org/10.1016/j.gloenvcha.2015.06.004>, <http://dx.doi.org/10.1016/j.gloenvcha.2015.06.004>, 2017.
- Di Marco, M., Harwood, T. D., Hoskins, A. J., Ware, C., Hill, S. L. L., and Ferrier, S.: Projecting impacts of global climate and land-use scenarios on plant biodiversity using compositional-turnover modelling, *Global Change Biology*, 1, 173–16, <https://doi.org/10.1111/gcb.14663>, <https://onlinelibrary.wiley.com/doi/abs/10.1111/gcb.14663>, 2019.
- 490 Doelman, J. C., Stehfest, E., Tabeau, A., van Meijl, H., Lassaletta, L., Gernaat, D. E. H. J., Hermans, K., Harmsen, M., Daioglou, V., Biemans, H., van der Sluis, S., and van Vuuren, D. P.: Exploring SSP land-use dynamics using the IMAGE model: Regional and gridded scenarios of land-use change and land-based climate change mitigation, *Global Environmental Change-Human and Policy Dimensions*, 48, 119–135, <https://doi.org/10.1016/j.gloenvcha.2017.11.014>, <https://doi.org/10.1016/j.gloenvcha.2017.11.014>, 2018.
- 495 Dufresne, J. L., Foujols, M. A., Denvil, S., Caubel, A., Marti, O., Aumont, O., Balkanski, Y., Bekki, S., Bellenger, H., Benshila, R., Bony, S., Bopp, L., Braconnot, P., Brockmann, P., Cadule, P., Cheruy, F., Codron, F., Cozic, A., Cugnet, D., de Noblet, N., Duvel, J. P., Ethé, C., Fairhead, L., Fichefet, T., Flavoni, S., Friedlingstein, P., Grandpeix, J. Y., Guez, L., Guilyardi, E., Hauglustaine, D., Hourdin, F., Idelkadi, A., Ghattas, J., Joussaume, S., Kageyama, M., Krinner, G., Labetoulle, S., Lahellec, A., Lefebvre, M. P., Lefevre, F., Levy, C., Li, Z. X., Lloyd, J., Lott, F., Madec, G., Mancip, M., Marchand, M., Masson, S., Meurdesoif, Y., Mignot, J., Musat, I., Parouty, S., Polcher, J., Rio, C., Schulz, M., Swingedouw, D., Szopa, S., Talandier, C., Terray, P., Viovy, N., and Vuichard, N.: Climate change projections using the IPSL-CM5 Earth System Model: from CMIP3 to CMIP5, *Climate Dynamics*, 40, 2123–2165, <https://doi.org/10.1007/s00382-012-1636-1>, 2013.
- 500 Ebi, K. L. and McGregor, G.: Climate Change, Tropospheric Ozone and Particulate Matter, and Health Impacts, *Environmental Health Perspectives*, 116, 1449–1455, <https://doi.org/10.1289/ehp.11463>, <https://ehp.niehs.nih.gov/doi/10.1289/ehp.11463>, 2008.
- 505 Eitelberg, D. A., van Vliet, J., Doelman, J. C., Stehfest, E., and Verburg, P. H.: Demand for biodiversity protection and carbon storage as drivers of global land change scenarios, *Global Environmental Change-Human and Policy Dimensions*, 40, 101–111, <https://doi.org/10.1016/j.gloenvcha.2016.06.014>, <http://dx.doi.org/10.1016/j.gloenvcha.2016.06.014>, 2016.
- Elliott, J., Deryng, D., Müller, C., Frieler, K., Konzmann, M., Gerten, D., Glotter, M., Flörke, M., Wada, Y., Best, N., Eisner, S., Fekete, B. M., Folberth, C., Foster, I., Gosling, S. N., Haddeland, I., Khabarov, N., Ludwig, F., Masaki, Y., Olin, S., Rosenzweig, C., Ruane, A. C., Satoh, Y., Schmid, E., Stacke, T., Tang, Q., and Wisser, D.: Constraints and potentials of future irrigation water availability on agricultural production under climate change., *Proceedings of the National Academy of Sciences*, 111, 3239–3244, <https://doi.org/10.1073/pnas.1222474110>, <http://www.pnas.org/lookup/doi/10.1073/pnas.1222474110>, 2014.
- 510 Elliott, J., Müller, C., Deryng, D., Chryssanthacopoulos, J., Boote, K. J., Büchner, M., Foster, I., Glotter, M., Heinke, J., Iizumi, T., Izaurralde, R. C., Mueller, N. D., Ray, D. K., Rosenzweig, C., Ruane, A. C., and Sheffield, J.: The Global Gridded Crop Model Intercomparison: data and modeling protocols for Phase 1 (v1.0), *Geoscientific Model Development*, 8, 261–277, <https://doi.org/10.5194/gmd-8-261-2015>, <http://www.geosci-model-dev.net/8/261/2015/>, 2015.
- 515 Engström, K., Olin, S., Rounsevell, M. D. A., Brogaard, S., van Vuuren, D. P., Alexander, P., Murray-Rust, D., and Arneeth, A.: Assessing uncertainties in global cropland futures using a conditional probabilistic modelling framework, *Earth System Dynamics*, 7, 893–915, <https://doi.org/10.5194/esd-7-893-2016>, <http://www.earth-syst-dynam.net/7/893/2016/>, 2016a.
- 520 Engström, K., Rounsevell, M. D. A., Murray-Rust, D., Hardacre, C., Alexander, P., Cui, X., Palmer, P. I., and Arneeth, A.: Applying Occam’s razor to global agricultural land use change, *Environmental Modelling and Software*, 75, 212–229, <https://doi.org/10.1016/j.envsoft.2015.10.015>, <http://dx.doi.org/10.1016/j.envsoft.2015.10.015>, 2016b.



- FAO STAT: Commodity Balances/Crops Primary Equivalent (2018-09-24), Food and Agriculture Organization of the United Nations, 2018a.
- FAO STAT: Commodity Balances/Livestock and Fish Primary Equivalent (2018-09-24), Food and Agriculture Organization of the United Nations, 2018b.
- 525 FAO STAT: Food Supply (2018-09-24), Food and Agriculture Organization of the United Nations, 2018c.
- Feng, Z. and Kobayashi, K.: Assessing the impacts of current and future concentrations of surface ozone on crop yield with meta-analysis, *Atmospheric Environment*, 43, 1510–1519, <https://doi.org/10.1016/j.atmosenv.2008.11.033>, <http://dx.doi.org/10.1016/j.atmosenv.2008.11.033>, 2009.
- 530 Fowler, D., Pilegaard, K., Sutton, M. A., Ambus, P., Raivonen, M., Duyzer, J., Simpson, D., Fagerli, H., Fuzzi, S., Schjoerring, J. K., Granier, C., Nefel, A., Isaksen, I. S. A., Laj, P., Maione, M., Monks, P. S., Burkhardt, J., Daemmgen, U., Neirynck, J., Personne, E., Wichink-Kruit, R., Butterbach-Bahl, K., Flechard, C., Tuovinen, J. P., Coyle, M., Gerosa, G., Loubet, B., Altimir, N., Gruenhage, L., Ammann, C., Cieslik, S., Paoletti, E., Mikkelsen, T. N., Ro-Poulsen, H., Cellier, P., Cape, J. N., Horvath, L., Loreto, F., Niinemets, U., Palmer, P. I., Rinne, J., Misztal, P., Nemitz, E., Nilsson, D., Pryor, S., Gallagher, M. W., Vesala, T., Skiba, U., Brüggemann, N., Zechmeister-Boltenstern, S., Williams, J., Dowd, C. O., Facchini, M. C., de Leeuw, G., Flossman, A., Chaumerliac, N., and Erisman, J. W.: Atmospheric composition change: Ecosystems–Atmosphere interactions, *Atmospheric Environment*, 43, 5193–5267, <https://doi.org/10.1016/j.atmosenv.2009.07.068>, <http://dx.doi.org/10.1016/j.atmosenv.2009.07.068>, 2009.
- Gerten, D., Schaphoff, S., Haberlandt, U., Lucht, W., and Sitch, S.: Terrestrial vegetation and water balance—hydrological evaluation of a dynamic global vegetation model, *Journal of Hydrology*, 286, 249–270, <https://doi.org/10.1016/j.jhydrol.2003.09.029>, <https://linkinghub.elsevier.com/retrieve/pii/S0022169403003901>, 2004.
- 540 Haddeland, I., HEINKE, J., Biemans, H., Eisner, S., Flörke, M., Hanasaki, N., Konzmann, M., Ludwig, F., Masaki, Y., Schewe, J., Stacke, T., Tessler, Z. D., Wada, Y., and Wissler, D.: Global water resources affected by human interventions and climate change, *Proceedings of the National Academy of Sciences of the United States of America*, 111, 3251–3256, <https://doi.org/10.1073/pnas.1222475110>, <http://www.pnas.org/lookup/doi/10.1073/pnas.1222475110>, 2014.
- 545 Hantson, S., Knorr, W., Schurgers, G., Pugh, T. A. M., and Arneth, A.: Global isoprene and monoterpene emissions under changing climate, vegetation, CO₂ and land use, *Atmospheric Environment*, 155, 35–45, <https://doi.org/10.1016/j.atmosenv.2017.02.010>, <http://dx.doi.org/10.1016/j.atmosenv.2017.02.010>, 2017.
- Harris, I., Jones, P. D., Osborn, T. J., and Lister, D. H.: Updated high-resolution grids of monthly climatic observations - the CRU TS3.10 Dataset, *International Journal of Climatology*, 34, 623–642, <https://doi.org/10.1002/joc.3711>, <http://doi.wiley.com/10.1002/joc.3711>, 2014.
- 550 Henry, R. C., Alexander, P., Rabin, S. S., Anthoni, P., Rounsevell, M. D. A., and Arneth, A.: The role of global dietary transitions for safeguarding biodiversity (in review), 2019.
- Hof, C., Voskamp, A., Biber, M. F., Böhning-Gaese, K., Engelhardt, E. K., Niamir, A., Willis, S. G., and Hickler, T.: Bioenergy cropland expansion may offset positive effects of climate change mitigation for global vertebrate diversity, *Proceedings of the National Academy of Sciences of the United States of America*, 10, 201807745–6, <https://doi.org/10.1073/pnas.1807745115>, <http://www.pnas.org/lookup/doi/10.1073/pnas.1807745115>, 2018.
- 555 Humpenöder, F., Popp, A., Dietrich, J. P., Klein, D., Lotze-Campen, H., Bonsch, M., Bodirsky, B. L., Weindl, I., Stevanovic, M., and Müller, C.: Investigating afforestation and bioenergy CCS as climate change mitigation strategies, pp. 1–14, <https://doi.org/10.1088/1748-9326/9/6/064029>, 2014.



- 560 Hurtt, G. C., Chini, L. P., Frohking, S., Betts, R. A., Feddema, J., Fischer, G., Fisk, J. P., Hibbard, K., Houghton, R. A., Janetos, A., Jones, C. D., Kindermann, G., Kinoshita, T., Klein Goldewijk, K., Riahi, K., Shevliakova, E., Smith, S., Stehfest, E., Thomson, A., Thornton, P., van Vuuren, D. P., and Wang, Y. P.: Harmonization of land-use scenarios for the period 1500–2100: 600 years of global gridded annual land-use transitions, wood harvest, and resulting secondary lands, *Climatic Change*, 109, 117–161, <https://doi.org/10.1007/s10584-011-0153-2>, <http://link.springer.com/10.1007/s10584-011-0153-2>, 2011.
- 565 IIASA: SSP Database (version 0.93), International Institute for Applied Systems Analysis, 2014.
IPBES: Summary for Policymakers of the Regional Assessment Report on Biodiversity and Ecosystem Services for Europe and Central Asia, Tech. rep., Bonn, Germany, 2018a.
IPBES: Summary for policymakers of the regional assessment report on biodiversity and ecosystem services for the Americas of the Intergovernmental Science-Policy Platform on Biodiversity and Ecosystem Services, Tech. rep., BONN, GERMANY, 2018b.
- 570 Jantz, S. M., Barker, B., Brooks, T. M., Chini, L. P., Huang, Q., Moore, R. M., Noel, J., and Hurtt, G. C.: Future habitat loss and extinctions driven by land-use change in biodiversity hotspots under four scenarios of climate-change mitigation, *Conservation Biology*, 29, 1122–1131, <https://doi.org/10.1111/cobi.12549>, <http://doi.wiley.com/10.1111/cobi.12549>, 2015.
Jones, B. and O'Neill, B. C.: Spatially explicit global population scenarios consistent with the Shared Socioeconomic Pathways, *Environmental Research Letters*, 11, 084003, <https://doi.org/10.1088/1748-9326/11/8/084003>, <http://stacks.iop.org/1748-9326/11/i=8/a=084003?key=crossref.51e5432142aaf508d829ebd92d31e7ca>, 2016.
- 575 KC, S. and Lutz, W.: The human core of the shared socioeconomic pathways: Population scenarios by age, sex and level of education for all countries to 2100, *Global Environmental Change-Human and Policy Dimensions*, 42, 181–192, <https://doi.org/10.1016/j.gloenvcha.2014.06.004>, <http://dx.doi.org/10.1016/j.gloenvcha.2014.06.004>, 2017.
Kesselmeier, J. and Staudt, M.: Biogenic Volatile Organic Compounds (VOC): An Overview on Emission, Physiology and Ecology, *Journal of Atmospheric Chemistry*, 33, 23–88, <https://doi.org/10.1023/A:1006127516791>, <https://link.springer.com/article/10.1023/A:1006127516791>, 1999.
- 580 Keyzer, M. A., Merbis, M. D., Pavel, I. F. P. W., and van Wesenbeeck, C. F. A.: Diet shifts towards meat and the effects on cereal use: can we feed the animals in 2030?, *Ecological Economics*, 55, 187–202, <https://doi.org/10.1016/j.ecolecon.2004.12.002>, <http://linkinghub.elsevier.com/retrieve/pii/S0921800904004100>, 2005.
- 585 Krause, A., Pugh, T. A. M., Bayer, A. D., Doelman, J. C., Humpenöder, F., Anthoni, P., Olin, S., Bodirsky, B. L., Popp, A., Stehfest, E., and Arneth, A.: Global consequences of afforestation and bioenergy cultivation on ecosystem service indicators, *Biogeosciences*, 14, 4829–4850, <https://doi.org/10.5194/bg-14-4829-2017>, <https://www.biogeosciences.net/14/4829/2017/>, 2017.
- Lawrence, P. J., Lawrence, D. M., and Hurtt, G. C.: Attributing the Carbon Cycle Impacts of CMIP5 Historical and Future Land Use and Land Cover Change in the Community Earth System Model (CESM1), *Journal of Geophysical Research: Biogeosciences*, 123, 1732–1755, <https://doi.org/10.1029/2017JG004348>, <http://doi.wiley.com/10.1029/2017JG004348>, 2018.
- 590 Le Quéré, C., Andrew, R. M., Canadell, J. G., Sitch, S., Korsbakken, J. I., Peters, G. P., Manning, A. C., Boden, T. A., Tans, P. P., Houghton, R. A., Keeling, R. F., Alin, S., Andrews, O. D., Anthoni, P., Barbero, L., Bopp, L., Chevallier, F., Chini, L. P., Ciais, P., Currie, K., Delire, C., Doney, S. C., Friedlingstein, P., Gkritzalis, T., Harris, I., Hauck, J., Haverd, V., Hoppema, M., Klein Goldewijk, K., Jain, A. K., Kato, E., Körtzinger, A., Landschützer, P., Lefèvre, N., Lenton, A., Lienert, S., Lombardozzi, D., Melton, J. R., Metzl, N., Millero, F., Monteiro, P. M. S., Munro, D. R., Nabel, J. E. M. S., Nakaoka, S.-i., O and apos Brien, K., Olsen, A., Omar, A. M., Ono, T., Pierrot, D., Poulter, B., Rödenbeck, C., Salisbury, J., Schuster, U., Schwinger, J., Séférian, R., Skjelvan, I., Stocker, B. D., Sutton, A. J., Takahashi, T., Tian, H., Tilbrook, B., van der Laan-Luijkx, I. T., van der Werf, G. R., Viovy, N., Walker, A. P., Wiltshire, A. J., and Zaehle, S.: Global Carbon



- Budget 2016, *Earth System Science Data*, 8, 605–649, <https://doi.org/10.5194/essd-8-605-2016>, <http://www.earth-syst-sci-data.net/8/605/2016/>, 2016.
- 600 Lindsokog, M., Arneth, A., Bondeau, A., Waha, K., Seaquist, J., Olin, S., and Smith, B.: Implications of accounting for land use in simulations of ecosystem carbon cycling in Africa, *Earth System Dynamics*, 4, 385–407, <https://doi.org/10.5194/esd-4-385-2013>, <http://www.earth-syst-dynam.net/4/385/2013/>, 2013.
- Mittermeier, R. A., Gil, P. R., Hoffmann, M., Pilgrim, J., Brooks, T. M., Mittermeier, C. G., Lamoreux, J., and da Fonseca, G. A. B.: Hotspots Revisited: Earth’s Biologically Richest and Most Endangered Terrestrial Ecoregions: Conservation International, Conservation International, [http://scholar.google.comjavascript:void\(0\)](http://scholar.google.comjavascript:void(0)), 2004.
- 605 Molotoks, A., Stehfest, E., Doelman, J., Albanito, F., Fitton, N., Dawson, T. P., and Smith, P.: Global projections of future cropland expansion to 2050 and direct impacts on biodiversity and carbon storage, *Global Change Biology*, 24, 5895–5908, <https://doi.org/10.1111/gcb.14459>, <http://doi.wiley.com/10.1111/gcb.14459>, 2018.
- Myers, N., Mittermeier, R. A., Mittermeier, C. G., da Fonseca, G. A. B., and Kent, J.: Biodiversity hotspots for conservation priorities, 610 *Nature*, 403, 853–858, <https://doi.org/10.1038/35002501>, <https://www.nature.com/articles/35002501>, 2000.
- Myers, S. S., Gaffikin, L., Golden, C. D., Ostfeld, R. S., Redford, K. H., Ricketts, T. H., Turner, W. R., and Osofsky, S. A.: Human health impacts of ecosystem alteration., *Proceedings of the National Academy of Sciences*, 110, 18 753–18 760, <https://doi.org/10.1073/pnas.1218656110>, <http://www.pnas.org/cgi/doi/10.1073/pnas.1218656110>, 2013.
- Myhre, G., Shindell, D. T., Bréon, F.-M., Collins, W., Fuglestedt, J., Huang, J., Koch, D., Lamarque, J.-F., Lee, D., Mendoza, B., Nakajima, 615 T., Robock, A., Stephens, G., and Zhang, H.: 8: Anthropogenic and natural radiative forcing, pp. 659–740, Cambridge, United Kingdom and New York, NY, USA, http://www.climatechange2013.org/images/report/WG1AR5_Chapter08_FINAL.pdf, 2013.
- Newbold, T., Hudson, L. N., Hill, S. L. L., Contu, S., Lysenko, I., Senior, R. A., Börger, L., Bennett, D. J., Choimes, A., Collen, B., Day, J., De Palma, A., Díaz, S., Echeverria-Londoño, S., Edgar, M. J., Feldman, A., Garon, M., Harrison, M. L. K., Alhousseini, T., Ingram, D. J., Itescu, Y., Kattge, J., Kemp, V., Kirkpatrick, L., Kleyer, M., Correia, D. L. P., Martin, C. D., Meiri, S., Novosolov, M., Pan, Y., Phillips, 620 H. R. P., Purves, D. W., Robinson, A., Simpson, J., Tuck, S. L., Weiher, E., White, H. J., Ewers, R. M., Mace, G. M., Scharlemann, J. P. W., and Purvis, A.: Global effects of land use on local terrestrial biodiversity, *Nature*, 520, 45–50, <https://doi.org/10.1038/nature14324>, <http://www.nature.com/doi/10.1038/nature14324>, 2015.
- Nishina, K., Ito, A., Falloon, P., Friend, A. D., Beerling, D. J., Ciais, P., Clark, D. B., Kahana, R., Kato, E., Lucht, W., Lomas, M., Pavlick, R., Schaphoff, S., Warszawski, L., and Yokohata, T.: Decomposing uncertainties in the future terrestrial carbon budget associated with 625 emission scenarios, climate projections, and ecosystem simulations using the ISI-MIP results, *Earth System Dynamics*, 6, 435–445, <https://doi.org/10.5194/esd-6-435-2015>, <http://www.earth-syst-dynam.net/6/435/2015/>, 2015.
- Olin, S., Lindsokog, M., Pugh, T. A. M., Schurgers, G., Wårlind, D., Mishurov, M., Zaehle, S., Stocker, B. D., Smith, B., and Arneth, A.: Soil carbon management in large-scale Earth system modelling: implications for crop yields and nitrogen leaching, *Earth System Dynamics*, 6, 745–768, <https://doi.org/10.5194/esd-6-745-2015>, <http://www.earth-syst-dynam.net/6/745/2015/>, 2015a.
- 630 Olin, S., Schurgers, G., Lindsokog, M., Wårlind, D., Smith, B., Bodin, P., Holmér, J., and Arneth, A.: Modelling the response of yields and tissue C : N to changes in atmospheric CO₂ and N management in the main wheat regions of western Europe, *Biogeosciences*, 12, 2489–2515, <https://doi.org/10.5194/bg-12-2489-2015>, <http://www.biogeosciences.net/12/2489/2015/>, 2015b.
- Olson, D. M., Dinerstein, E., Wikramanayake, E. D., Burgess, N. D., Powell, G. V. N., Underwood, E. C., D’Amico, J. A., Itoua, I., Strand, H. E., Morrison, J. C., Loucks, C. J., Allnutt, T. F., Ricketts, T. H., Kura, Y., Lamoreux, J. F., Wettengel, W. W., Hedao, P., and Kassem,



- 635 K. R.: Terrestrial Ecoregions of the World: A New Map of Life on Earth, *BioScience*, 51, 933–938, <https://academic.oup.com/bioscience/article-abstract/51/11/933/227116>, 2001.
- O'Neill, B. C., Kriegler, E., Riahi, K., Ebi, K. L., Hallegatte, S., Carter, T. R., Mathur, R., and van Vuuren, D. P.: A new scenario framework for climate change research: the concept of shared socioeconomic pathways, *Climatic Change*, 122, 387–400, <https://doi.org/10.1007/s10584-013-0905-2>, <http://link.springer.com/10.1007/s10584-013-0905-2>, 2014.
- 640 O'Neill, B. C., Kriegler, E., Ebi, K. L., Kemp-Benedict, E., Riahi, K., Rothman, D. S., van Ruijven, B. J., van Vuuren, D. P., Birkmann, J., Kok, K., Levy, M., and Solecki, W.: The roads ahead: Narratives for shared socioeconomic pathways describing world futures in the 21st century, *Global Environmental Change-Human and Policy Dimensions*, pp. 1–12, <https://doi.org/10.1016/j.gloenvcha.2015.01.004>, <http://dx.doi.org/10.1016/j.gloenvcha.2015.01.004>, 2015.
- Popp, A., Calvin, K., Fujimori, S., Havlik, P., Humpenöder, F., Stehfest, E., Bodirsky, B. L., Dietrich, J. P., Doelmann, J. C., Gusti, M., Hasegawa, T., Kyle, P., Obersteiner, M., Tabeau, A., Takahashi, K., Valin, H., Waldhoff, S., Weindl, I., Wise, M., Kriegler, E., Lotze-Campen, H., Fricko, O., Riahi, K., and van Vuuren, D. P.: Land-use futures in the shared socio-economic pathways, *Global Environmental Change-Human and Policy Dimensions*, 42, 331–345, <https://doi.org/10.1016/j.gloenvcha.2016.10.002>, <http://dx.doi.org/10.1016/j.gloenvcha.2016.10.002>, 2017.
- Portmann, F. T., Siebert, S., and Döll, P.: MIRCA2000—Global monthly irrigated and rainfed crop areas around the year
650 2000: A new high-resolution data set for agricultural and hydrological modeling, *Global Biogeochemical Cycles*, 24, n/a–n/a, <https://doi.org/10.1029/2008GB003435>, <http://doi.wiley.com/10.1029/2008GB003435>, 2010.
- Quesada, B., Arneeth, A., and de Noblet-Ducoudré, N.: Atmospheric, radiative, and hydrologic effects of future land use and land cover changes: A global and multimodel climate picture, *Journal of Geophysical Research: Atmospheres*, 122, 5113–5131, <https://doi.org/10.1002/2016JD025448>, <http://doi.wiley.com/10.1002/2016JD025448>, 2017.
- 655 Rabin, S. S.: Harmonizing LandSyMM with historical data, p. 3, <https://doi.org/10.5281/zenodo.3336129>, <https://github.com/samsrabin/harmonizing-LU-mgmt/blob/master/README.md>, 2019.
- Rap, A., Scott, C. E., Reddington, C. L., Mercado, L., Ellis, R. J., Garraway, S., Evans, M. J., Beerling, D. J., MacKenzie, A. R., Hewitt, C. N., and Spracklen, D. V.: Enhanced global primary production by biogenic aerosol via diffuse radiation fertilization, *Nature Publishing Group*, pp. 1–7, <https://doi.org/10.1038/s41561-018-0208-3>, <http://dx.doi.org/10.1038/s41561-018-0208-3>, 2018.
- 660 Rockström, J., Steffen, W., Noone, K., Persson, Å., Chapin III, F. S., Lambin, E. F., Lenton, T. M., Scheffer, M., Folke, C., Schnellhuber, H. J., Nykvist, B., de Wit, C. A., Hughes, T., van der Leeuw, S., Rodhe, H., Sörlin, S., Snyder, P. K., Costanza, R., Svedin, U., Falkenmark, M., Karlberg, L., Corell, R. W., Fabry, V. J., Hansen, J., Walker, B., Liverman, D., Richardson, K., Crutzen, P., and Foley, J. A.: A safe operating space for humanity, *Nature*, 461, <https://doi.org/10.1038/461472a>, <https://www.nature.com/articles/461472a>, 2009.
- Rogelj, J., Shindell, D. T., Jiang, K., Fifita, S., Forster, P., Ginzburg, V., Handa, C., Khesghi, H., Kobayashi, S., Kriegler, E., Mundaca,
665 L., Séférian, R., and Vilariño, M. V.: 2: Mitigation pathways compatible with 1.5°C in the context of sustainable development, in: *Global warming of 1.5°C: An IPCC Special Report on the impacts of global warming of 1.5°C above pre-industrial levels and related global greenhouse gas emission pathways, in the context of strengthening the global response to the threat of climate change, sustainable development, and efforts to eradicate poverty*, edited by Masson-Delmotte, V., Zhai, P., Pörtner, H. O., ROBERTS, D., Skea, J., Shukla, P. R., Pirani, A., Moufouma-Okia, W., Péan, C., Pidcock, R., Connors, S., Matthews, J. B. R., Chen, Y., Zhou, X., Gomis, M. I., Lonnoy, E., Maycock, T.,
670 Tignor, M., and Waterfield, T., pp. 93–174, Cambridge, United Kingdom and New York, NY, USA, <https://www.ipcc.ch/sr15/chapter/2-0/>, 2018.



- Rosenkranz, M., Pugh, T. A. M., Schnitzler, J.-P., and Arneth, A.: Effect of land-use change and management on biogenic volatile organic compound emissions - selecting climate-smart cultivars, *Plant, Cell and Environment*, 38, 1896–1912, <https://doi.org/10.1111/pce.12453>, <http://doi.wiley.com/10.1111/pce.12453>, 2014.
- 675 Rosenzweig, C., Jones, J. W., Hatfield, J. L., Ruane, A. C., Boote, K. J., Thorburn, P., Antle, J. M., Nelson, G. C., Porter, C., Janssen, S., Asseng, S., Basso, B., Ewert, F., Wallach, D., Baigorria, G., and Winter, J. M.: The Agricultural Model Inter-comparison and Improvement Project (AgMIP): Protocols and pilot studies, *Agricultural and Forest Meteorology*, 170, 166–182, <https://doi.org/10.1016/j.agrformet.2012.09.011>, <http://dx.doi.org/10.1016/j.agrformet.2012.09.011>, 2013.
- Schurgers, G., Arneth, A., Holzinger, R., and Goldstein, A. H.: Process-based modelling of biogenic monoterpene emissions combining production and release from storage, *Atmospheric Chemistry and Physics*, 9, 3409–3423, <https://doi.org/10.5194/acp-9-3409-2009>, <http://www.atmos-chem-phys.net/9/3409/2009/>, 2009.
- Shcherbak, I., Millar, N., and Robertson, G. P.: Global metaanalysis of the nonlinear response of soil nitrous oxide (N₂O) emissions to fertilizer nitrogen., *Proceedings of the National Academy of Sciences*, 111, 9199–9204, <https://doi.org/10.1073/pnas.1322434111>, <http://www.pnas.org/cgi/doi/10.1073/pnas.1322434111>, 2014.
- 685 Simpson, R. D., Sedjo, R. A., and Reid, J. W.: Valuing Biodiversity for Use in Pharmaceutical Research, *Journal of Political Economy*, 104, 163–185, <https://doi.org/10.1086/262021>, <https://www.journals.uchicago.edu/doi/10.1086/262021>, 1996.
- Smith, B., Prentice, I. C., and Sykes, M. T.: Representation of vegetation dynamics in the modelling of terrestrial ecosystems: comparing two contrasting approaches within European climate space, *Global Ecology and Biogeography*, 10, 621–637, <https://doi.org/10.1046/j.1466-822X.2001.t01-1-00256.x>, <http://onlinelibrary.wiley.com/doi/10.1046/j.1466-822X.2001.t01-1-00256.x/full>, 2001.
- 690 Smith, B., Wårlind, D., Arneth, A., Hickler, T., Leadley, P., Siltberg, J., and Zaehle, S.: Implications of incorporating N cycling and N limitations on primary production in an individual-based dynamic vegetation model, *Biogeosciences*, 11, 2027–2054, <https://doi.org/10.5194/bg-11-2027-2014>, <http://www.biogeosciences.net/11/2027/2014/>, 2014.
- Sporre, M. K., Blichner, S. M., Karset, I. H. H., Makkonen, R., and Berntsen, T. K.: BVOC–aerosol–climate feedbacks investigated using NorESM, *Atmospheric Chemistry and Physics*, 19, 4763–4782, <https://doi.org/10.5194/acp-19-4763-2019>, <https://www.atmos-chem-phys.net/19/4763/2019/>, 2019.
- 695 Szogs, S., Arneth, A., Anthoni, P., Doelman, J. C., Humpenöder, F., Popp, A., Pugh, T. A. M., and Stehfest, E.: Impact of LULCC on the emission of BVOCs during the 21st century, *Atmospheric Environment*, 165, 73–87, <https://doi.org/10.1016/j.atmosenv.2017.06.025>, <http://dx.doi.org/10.1016/j.atmosenv.2017.06.025>, 2017.
- Taylor, K. E., Stouffer, R. J., and Meehl, G. A.: An Overview of CMIP5 and the Experiment Design, *Bulletin of the American Meteorological Society*, 93, 485–498, <https://doi.org/10.1175/BAMS-D-11-00094.1>, <http://journals.ametsoc.org/doi/abs/10.1175/BAMS-D-11-00094.1>, 2012.
- 700 Tilman, D., Balzer, C., Hill, J., and Befort, B. L.: Global food demand and the sustainable intensification of agriculture, *Proceedings of the National Academy of Sciences*, 108, 20 260–20 264, <https://doi.org/10.1073/pnas.1116437108/-DCSupplemental/pnas.201116437SI.pdf>, <http://www.pnas.org/content/108/50/20260.short>, 2011.
- 705 Tilman, D., Isbell, F., and Cowles, J. M.: Biodiversity and Ecosystem Functioning, *Annual Review of Ecology, Evolution, and Systematics*, 45, 471–493, <https://doi.org/10.1146/annurev-ecolsys-120213-091917>, <http://www.annualreviews.org/doi/10.1146/annurev-ecolsys-120213-091917>, 2014.



- van Vuuren, D. P., Edmonds, J., Kainuma, M., Riahi, K., Thomson, A., Hibbard, K., Hurtt, G. C., Kram, T., Krey, V., Lamarque, J.-F., Masui, T., Meinshausen, M., Nakicenovic, N., Smith, S. J., and Rose, S. K.: The representative concentration pathways: an overview, *Climatic Change*, 109, 5–31, <https://doi.org/10.1007/s10584-011-0148-z>, <http://link.springer.com/10.1007/s10584-011-0148-z>, 2011.
- 710 van Vuuren, D. P., Stehfest, E., Gernaat, D. E. H. J., Berg, M., Bijl, D. L., Boer, H. S., Daioglou, V., Doelman, J. C., Edelenbosch, O. Y., Harmsen, M., Hof, A. F., and Sluiseveld, M. A. E.: Alternative pathways to the 1.5°C target reduce the need for negative emission technologies, *Nature Publishing Group*, pp. 1–10, <https://doi.org/10.1038/s41558-018-0119-8>, <http://dx.doi.org/10.1038/s41558-018-0119-8>, 2018.
- 715 Verhagen, W., van der Zanden, E. H., Strauch, M., van Teeffelen, A. J. A., and Verburg, P. H.: Optimizing the allocation of agri-environment measures to navigate the trade-offs between ecosystem services, biodiversity and agricultural production, *Environmental Science and Policy*, 84, 186–196, <https://doi.org/10.1016/j.envsci.2018.03.013>, <https://doi.org/10.1016/j.envsci.2018.03.013>, 2018.
- Vitousek, P. M., Aber, J. D., Howarth, R. W., Likens, G. E., Matson, P. A., Schindler, D. W., Schlesinger, W. H., and Tilman, D. G.: Human Alteration of the Global Nitrogen Cycle: Sources and Consequences, *Ecological Applications*, 7, 737–750, <https://doi.org/10.2307/2269431>,
720 <http://www.jstor.org/stable/2269431?origin=crossref>, 1997.
- Weindl, I., Popp, A., Bodirsky, B. L., Rolinski, S., Lotze-Campen, H., Biewald, A., Humpenöder, F., Dietrich, J. P., and Stevanovic, M.: Livestock and human use of land: Productivity trends and dietary choices as drivers of future land and carbon dynamics, *Global and Planetary Change*, 159, 1–10, <https://doi.org/10.1016/j.gloplacha.2017.10.002>, <https://doi.org/10.1016/j.gloplacha.2017.10.002>, 2017.
- Wheater, H. and Evans, E.: Land use, water management and future flood risk, *Land Use Policy*, 26, S251–S264,
725 <https://doi.org/10.1016/j.landusepol.2009.08.019>, <http://linkinghub.elsevier.com/retrieve/pii/S0264837709001082>, 2009.
- Wilhite, D. A. and Glantz, M. H.: Understanding: the drought phenomenon: the role of definitions, *Water International*, 10, 111–120, <https://doi.org/10.1080/02508068508686328>, <https://www.tandfonline.com/doi/pdf/10.1080/02508068508686328>, 1985.
- Yang, W. and Omaye, S. T.: Air pollutants, oxidative stress and human health, *Mutation Research/Genetic Toxicology and Environmental Mutagenesis*, 674, 45–54, <https://doi.org/10.1016/j.mrgentox.2008.10.005>, <https://linkinghub.elsevier.com/retrieve/pii/S1383571808003045>,
730 2009.
- Young, P. J., Arneth, A., Schurgers, G., Zeng, G., and Pyle, J. A.: The CO₂ inhibition of terrestrial isoprene emission significantly affects future ozone projections, *Atmospheric Chemistry and Physics*, 9, 2793–2803, <https://doi.org/10.5194/acp-9-2793-2009>, <http://www.atmos-chem-phys.net/9/2793/2009/>, 2009.
- Zhang, B., Tian, H., Lu, C., Dangal, S. R. S., Yang, J., and Pan, S.: Global manure nitrogen production and application in crop-
735 land during 1860–2014: a 5arcmin gridded global dataset for Earth system modeling, *Earth System Science Data*, 9, 667–678, <https://doi.org/10.5194/essd-9-667-2017>, <https://www.earth-syst-sci-data.net/9/667/2017/>, 2017.